



Cy 74

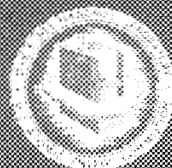
A Model to Calculate Mass Flow Rate and Other Quantities of Two-Phase Flow in a Pipe with a Densitometer, a Drag Disk, and a Turbine Meter

Izuo Aya

OAK RIDGE NATIONAL LABORATORY
CENTRAL RESEARCH LIBRARY
DOCUMENT COLLECTION
LIBRARY LOAN COPY

DO NOT TRANSFER TO ANOTHER PERSON

If you wish someone else to see this
document, send in name with document
and the library will arrange a loan.



OAK RIDGE NATIONAL LABORATORY
OPERATED BY UNION CARBIDE CORPORATION • FOR THE U.S. ATOMIC ENERGY COMMISSION

Printed in the United States of America. Available from
National Technical Information Service
U.S. Department of Commerce
5285 Port Royal Road, Springfield, Virginia 22161
Price: Printed Copy \$5.45; Microfiche \$2.25

This report was prepared as an account of work sponsored by the United States Government. Neither the United States nor the Energy Research and Development Administration, nor any of their employees, nor any of their contractors, subcontractors, or their employees, makes any warranty, express or implied, or assumes any legal liability or responsibility for the accuracy, completeness or usefulness of any information, apparatus, product or process disclosed, or represents that its use would not infringe privately owned rights.

Contract No. W-7405-eng-26

Reactor Division

A MODEL TO CALCULATE MASS FLOW RATE AND OTHER QUANTITIES
OF TWO-PHASE FLOW IN A PIPE WITH A DENSITOMETER,
A DRAG DISK, AND A TURBINE METER

Izuo Aya

NOVEMBER 1975

NOTICE: This document contains information of a preliminary nature and was prepared primarily for internal use at the Oak Ridge National Laboratory. It is subject to revision or correction and therefore does not represent a final report.

OAK RIDGE NATIONAL LABORATORY
Oak Ridge, Tennessee 37830
operated by
UNION CARBIDE CORPORATION
for the
U.S. ENERGY RESEARCH AND DEVELOPMENT ADMINISTRATION

OAK RIDGE NATIONAL LABORATORY LIBRARIES



3 4456 0550492 3

TABLE OF CONTENTS

	<u>Page</u>
ABSTRACT	1
1. INTRODUCTION	2
2. ANALYSIS	4
2.1 Densitometer	4
2.2 Drag Disk	5
2.3 Turbine Meter	6
3. COMPARISON OF PROPOSED MODEL WITH HOMOGENEOUS FLOW AND OTHER MODELS	8
3.1 Comparison with Homogeneous Flow	8
3.2 Comparison with Homogeneous Model (INEL Method)	10
3.3 Comparison with Popper's Model	12
3.4 Comparison with Rouhani's Model	14
4. COMPARISON OF FOUR TURBINE METER MODELS WITH ROUHANI'S DATA	15
4.1 Void Fraction	16
4.2 Mass Flow Rate	18
5. CONSIDERATIONS IN THE USE OF THIS MODEL	22
6. CONCLUSION	23
ACKNOWLEDGMENT	23
NOMENCLATURE	24
REFERENCES	55

A MODEL TO CALCULATE MASS FLOW RATE AND OTHER QUANTITIES
OF TWO-PHASE FLOW IN A PIPE WITH A DENSITOMETER,
A DRAG DISK, AND A TURBINE METER

Izuo Aya^{*}

ABSTRACT

The proposed model was developed at ORNL to calculate mass flow rate and other quantities of two-phase flow in a pipe when the flow is dispersed with slip between the phases. The calculational model is based on assumptions concerning the characteristics of a turbine meter and a drag disk. The model should be validated with experimental data before being used in blowdown analysis.

In order to compare dispersed flow and homogeneous flow, the ratio of readings from each flow regime for each device discussed here is calculated for a given mass flow rate and steam quality.

The sensitivity analysis shows that the calculated flow rate of a steam-water mixture (based on the measurements of a drag disk and a gamma densitometer in which the flow is assumed to be homogeneous even if there is some slip between phases) is very close to the real flow rate in the case of dispersed flow at a low quality. However, it is shown that the measurement with a turbine meter and a densitometer overestimates the flow rate at low and middle qualities and underestimates it at high quality.

The model is also compared with the methods of Rouhani and Popper used to measure the void fraction with one and two turbine meters respectively.

The comparison with Rouhani's experimental data of a turbine meter in vertical upflow in a straight tube shows that there are no significant differences among the models for the estimation of void fraction. These four models yield average errors between -1.4 and 3.8%. However, there are large differences in the calculation of mass flow rate. At a steam quality below 5% and a slip ratio below 4.5, Rouhani's method predicts flow rate the best. The homogeneous model and Popper's model overestimate less than 11%, and the proposed model underestimates by 5 to 11%. As the steam quality increases at a constant slip ratio, all models are prone to overestimate. At 20% quality the overestimates reach 8% in the proposed model, 15% in Rouhani's model, 38% in homogeneous model, and 57% in Popper's model.

* Assigned to Oak Ridge National Laboratory from Nuclear Ship Division, Ship Research Institute, Tokyo, Japan.

1. INTRODUCTION

Many experiments designed to improve the understanding of the transient behavior of a PWR or a BWR core during simultaneous loss-of-pressure and loss-of-coolant accidents have been done and are planned in the U. S. and other countries. In conducting such experiments, it is necessary to measure mass flow rate and steam quality in the break pipe and in the intact pipes of the primary loop. The measurements of mass flow rate and quality are used in assessing the mass and enthalpy balances of the loop. These measurements provide very important information, such as the water level in the pressure vessel, which largely controls the thermal condition of fuel rods or electric heaters.

It seems possible to determine the mass flow rate from the pressure vessel during blowdown by measuring the variation of the vessel weight.¹ The up-and-down motion of the vessel contents produces vertical forces which are superimposed on the vessel weight. To determine the mass flow rate, it is necessary to smooth the test curve; hence, short-term (<1-sec) mass flow rates cannot be determined by measuring the course of vessel weight with time. An orifice plate,²⁻⁵ a venturimeter,² or a nozzle^{5,6} may also be used. To determine mass flow rate and quality with these methods during a fast transient, correlations established for steady-state two-phase flow might be invalid or their accuracy decreased. Another possible difficulty in using these devices is that the fluid used to transfer the differential pressure to a measuring device might not be able to keep up with the fast depressurization and might boil.

In general, for the indirect determination of mass flow rate and quality, three independent measured variables are needed in addition to pressure and temperature. Thom⁷ noted that at each selected pressure, the slip ratio of steam-water two-phase flow may be taken as almost constant and independent of quality (Fig. 1). If this correlation is valid in the case of blowdown, the number of independent variables is reduced to two. Since the error shown in Fig. 4 of Ref. 7 is around $\pm 10\%$ in the pressure range from 115 to 2000 psia, all three independent measurements may be needed.

In the PWR Blowdown Heat Transfer Separate-Effects Program at ORNL, three measured variables — the apparent density from a gamma densitometer, a flow velocity from a turbine meter, and the momentum flux from a drag disk — are used in the determination of the flow rate and the steam quality. In principle, it is possible to determine the unknown variables from the three independent measured variables. However, it might be rather difficult and troublesome to establish the correlation or the analytical relationship between known and unknown variables, as it could change for each different flow regime. This corresponds to the ANC report,⁸ which states that the deficiency of drag-disk-turbine flowmeters for two-phase flow may be due in part to lack of knowledge about the flow regimes. Moreover, the boundaries between regimes are rather vague and different for each researcher.⁹⁻¹¹ Recently, Tong* suggested that the difficulty might be reduced if dispersed flow could be produced and maintained artificially at measuring points in a pipe during blowdown without incurring great pressure changes. Consequently, ORNL decided to investigate screens for dispersing the flow. The results of these studies will be presented elsewhere.

Figure 2 shows the arrangement of the densitometer, drag disk, and turbine meter in an instrumented spool piece of the ORNL Thermal-Hydraulic Test Facility (THTF). The orientation of an instrumented spool piece is horizontal or vertical. Turbine meters and drag disks to be used in the THTF are bidirectional, since the flow direction could change during blowdown. Some means for dispersing the flow will be installed at each end of the spool piece.

The model presented here permits one to deduce the mass flow rate, quality, and slip ratio of dispersed two-phase flow by using a densitometer, a drag disk, and a turbine meter. The proposed model is based on the following major assumptions concerning the characteristics of a turbine meter and a drag disk.

1. The reading of a turbine meter is determined by a momentum balance on turbine blades due to velocity differences of the two phases and the turbine blade.

* L. S. Tong, Deputy Director, Reactor Safety Research Division, Nuclear Regulatory Commission.

2. Mass fluxes exerting forces on turbine blades are $\alpha \rho_g (V_g - V_t)$ and $(1 - \alpha) \rho_f (V_t - V_f)$ for the gas and liquid phases respectively.

3. Contributions of gas and liquid phases to momentum flux detected by a drag disk are $\alpha C_{dg} \rho_g V_g^2$ and $C_{df} (1 - \alpha) \rho_f V_f^2$ respectively.

2. ANALYSIS

Relationships among quantities that appear in the dispersed regime of two-phase flow in a pipe are derived theoretically in this section by using some assumptions of the hydrodynamic characteristics of a turbine meter and a drag disk. In this report, homogeneous two-phase flow is defined as a flow in which the two phases are uniformly distributed at any cross section in the pipe with no slip between phases. Dispersed flow is defined as a flow in which the two phases are uniformly distributed at any cross section in the pipe but slip occurs between phases. Before starting the analysis, it might be convenient to define the void fraction and the quality of two-phase flow. The void fraction is defined by

$$\alpha = \frac{A_g}{A} \quad , \quad (1)$$

where A is the cross section of the pipe and A_g is the part of the cross section occupied by the gas phase. The quality is expressed by

$$x = \frac{m_g}{m_g + m_f} \quad , \quad (2)$$

where m_g and m_f are the mass flow rates of gas and liquid respectively.

2.1 Densitometer

A gamma densitometer should show the correct apparent density of dispersed (or homogeneous) flow in a pipe during blowdown if it can keep pace with the fast density change. The time constant of 16 msec for densitometers used in the THTF seems to be small enough for accurate measurement of the apparent density during blowdown. The apparent density

is defined by

$$\rho_a = \alpha \rho_g + (1 - \alpha) \rho_f \quad , \quad (3)$$

where ρ_g and ρ_f are the densities of gas and liquid phases respectively.

2.2 Drag Disk

Although the two-dimensional velocity profile of dispersed two-phase flow might differ from that of single-phase flow,¹² the gas and liquid velocities acting on the drag disk target can be assumed to be almost the same as the mean gas and liquid velocities exerting forces on the blades of a turbine meter within the Reynolds number range where the flow is turbulent. Therefore, the same symbols (V_g for the gas velocity and V_f for the liquid velocity) will be used henceforth for both drag disk and turbine meter.

The momentum flux detected by a drag disk¹³ for dispersed flow can be expressed as

$$I_d = C_{dg} \alpha \rho_g V_g^2 + C_{df} (1 - \alpha) \rho_f V_f^2 \quad , \quad (4)$$

where C_{dg} and C_{df} are, respectively, the drag coefficients of a drag disk for the gas and the liquid phases. Using the ratio of drag coefficients of a drag disk, $\bar{C}_d = C_{df}/C_{dg}$, Eq. (4) may be rewritten as

$$I_d = C_{dg} \alpha \rho_g V_f^2 [S^2 + \bar{C}_d f (1 - \alpha)/\alpha] \quad , \quad (5)$$

where S is the slip ratio (V_g/V_f) and f is the density ratio (ρ_f/ρ_g). The drag coefficients C_{dg} and C_{df} should be taken from calibrational tests for the drag disk. From Eqs. (3) and (5), the void fraction and the slip ratio are readily converted to

$$\alpha = \frac{\rho_f - \rho_a}{\rho_f - \rho_g} \quad ,$$

$$1 - \alpha = \frac{\rho_a - \rho_g}{\rho_f - \rho_g} \quad , \quad (6)$$

and

$$S^2 = \frac{(\rho_f - \rho_g)(I_d/C_{dg}) - (\rho_a - \rho_g) \rho_f \bar{C}_d V_f^2}{(\rho_f - \rho_a) \rho_g V_f^2} \quad (7)$$

By using Eqs. (6) and (7) and the following general relationship of the slip ratio, the void fraction, and the quality,

$$\frac{1 - \alpha}{\alpha} = \frac{S}{f} \frac{1 - x}{x} \quad (8)$$

the quality is expressed as

$$\frac{1}{x} = 1 + \frac{\rho_f \rho_a - \rho_g}{\rho_g \rho_f - \rho_a} \times \sqrt{\frac{\rho_f - \rho_a}{\rho_f - \rho_g} \rho_g V_f^2 / \left(\frac{I_d}{C_{dg}} - \frac{\rho_a - \rho_g}{\rho_f - \rho_g} \rho_f \bar{C}_d V_f^2 \right)} \quad (9)$$

The mass flux G and the mass flow rate W can then be written as

$$G = \alpha \rho_g V_g + (1 - \alpha) \rho_f V_f \quad (10a)$$

$$= \sqrt{\frac{\rho_f - \rho_a}{\rho_f - \rho_g} \rho_g \left(\frac{I_d}{C_{dg}} - \frac{\rho_a - \rho_g}{\rho_f - \rho_g} \rho_f \bar{C}_d V_f^2 \right)} + \frac{\rho_a - \rho_g}{\rho_f - \rho_g} \rho_f V_f \quad (10b)$$

and

$$W = \frac{\pi}{4} D_i^2 G \quad (11)$$

where D_i is the inner diameter of the pipe.

2.3 Turbine Meter

A turbine blade rotates with angular velocity ω . The turning speed of a point on the turbine blade is given by

$$V_r = r\omega \quad (12)$$

where r is the distance from the axis of rotation.

Assume that the frictional forces exerting on turbine blades are negligible when compared to the forces due to momentum changes of fluids. The turning speed V_r is then equivalent for fluids to the imaginary velocity of a turbine meter defined by

$$V_t = V_r / \tan \phi \quad , \quad (13)$$

where ϕ is the twisting angle of a blade (see Fig. 3). V_t can be regarded as constant over a turbine blade and corresponds with the fluid velocity detected by a turbine meter, since the twisting angle is usually chosen so that

$$\tan \phi / r = \text{constant} \quad . \quad (14a)$$

When this is true,

$$V_t \propto \omega \quad . \quad (14b)$$

The gas phase velocity is usually greater than or equal to the liquid velocity in dispersed flow. Therefore, the reading of a turbine meter should be some value between the gas velocity and the liquid velocity. A momentum balance about the turbine blade segment gives

$$\alpha \rho_g (V_g - V_t)^2 \sin^2 \phi = \bar{C}_t \rho_f (1 - \alpha) (V_t - V_f)^2 \sin^2 \phi \quad , \quad (15)$$

where \bar{C}_t is the ratio of drag coefficients of a turbine blade for the liquid and gas phases (C_{tf}/C_{tg}). \bar{C}_t should also be taken from calibration tests for the turbine meter; \bar{C}_t might be near unity for bidirectional turbine meters, such as those to be used in the THTF. Equation (15) may be reduced to

$$\frac{V_f}{V_t} = \frac{1 + \sqrt{\bar{C}_t Y}}{S + \sqrt{\bar{C}_t Y}} \quad , \quad (16)$$

where

$$Y \equiv f \left(\frac{1 - \alpha}{\alpha} \right) = \frac{\rho_f}{\rho_g} \left(\frac{\rho_a - \rho_g}{\rho_f - \rho_a} \right) \quad .$$

This may then be combined with Eqs. (6) and (7), eliminating S , to yield

$$\begin{aligned}
(\bar{C}_d + \bar{C}_t) v_f^2 - 2 \left(\sqrt{\frac{\bar{C}_t}{Y}} + \bar{C}_t \right) v_t v_f + \left(\frac{1}{\sqrt{Y}} + \sqrt{\bar{C}_t} \right)^2 v_t^2 \\
- \left(\frac{\rho_f - \rho_g}{\rho_a - \rho_g} \right) \frac{1}{\rho_f} \frac{I_d}{C_{dg}} = 0 \quad . \quad (17)
\end{aligned}$$

This then reduces to

$$v_f = \begin{cases} a + b & , \quad S \leq \bar{C}_d \sqrt{Y/\bar{C}_t} \\ a - b & , \quad S > \bar{C}_d \sqrt{Y/\bar{C}_t} \end{cases} \quad , \quad (18)$$

where

$$a = \sqrt{\frac{\bar{C}_t}{Y}} \left(\frac{1 + \sqrt{\bar{C}_t Y}}{\bar{C}_d + \bar{C}_t} \right) v_t$$

and

$$b = \frac{1}{\bar{C}_d + \bar{C}_t} \left[(\bar{C}_d + \bar{C}_t) \left(\frac{\rho_f - \rho_g}{\rho_a - \rho_g} \right) \frac{I_d}{\rho_f C_{dg}} - \frac{\bar{C}_d}{Y} \left(1 + \sqrt{\bar{C}_t Y} \right)^2 v_t^2 \right]^{1/2} .$$

It is obvious from Eq. (18) that the liquid velocity is expressed with three measured variables — the apparent density ρ_a from a densitometer, the momentum flux I_d from a drag disk, and the velocity V_t from a turbine meter — and with the phase densities determined by the pressure and the temperature at the measuring point. Substituting the value of V_f calculated by Eq. (18) into Eqs. (7), (9), and (10b) gives the slip ratio, the quality, and the mass flux based on measured variables only.

3. COMPARISON OF PROPOSED MODEL WITH HOMOGENEOUS FLOW AND OTHER MODELS

3.1 Comparison with Homogeneous Flow

To compare the readings of the three measuring devices in dispersed flow with the readings in homogeneous flow, calculations are made for each flow regime with equivalent phase mass fluxes. In homogeneous flow, the

mass balance equations are written as

$$\begin{aligned} \alpha \rho_g V_g &= \alpha_0 \rho_g V_0 && \text{(gas phase)} \\ (1 - \alpha) \rho_f V_f &= (1 - \alpha_0) \rho_f V_0 && \text{(liquid phase)} \end{aligned} \quad (19)$$

where α_0 and V_0 are the void fraction and the velocity of homogeneous flow. The readings of the three devices in homogeneous flow for apparent density, momentum flux, and turbine meter velocity, respectively, are

$$\rho_{a0} = \alpha_0 \rho_g + (1 - \alpha_0) \rho_f, \quad (20)$$

$$I_{d0} = C_{dg} V_0^2 [\alpha_0 \rho_g + \bar{C}_d (1 - \alpha_0) \rho_f], \quad (21)$$

$$V_{t0} = V_0. \quad (22)$$

Using some relationships deduced in Sect. 2 and Eqs. (19) through (22), the reading ratio of each device becomes,

$$\frac{\rho_a}{\rho_{a0}} = \frac{1 + f (1 - \alpha)/\alpha S + (1 - \alpha)/\alpha}{S + f (1 - \alpha)/\alpha 1 + (1 - \alpha)/\alpha} \quad (23a)$$

$$= \frac{1 + S (1 - x)/x f + (1 - x)/x}{1 + (1 - x)/x f + S (1 - x)/x}, \quad (23b)$$

$$\frac{I_d}{I_{d0}} = \frac{S^2 + \bar{C}_d f (1 - \alpha)/\alpha}{S + \bar{C}_d f (1 - \alpha)/\alpha} \frac{1 + (1 - \alpha)/\alpha}{S + (1 - \alpha)/\alpha} \quad (24a)$$

$$= \frac{S + \bar{C}_d (1 - x)/x}{1 + \bar{C}_d (1 - x)/x} \frac{f/S + (1 - x)/x}{f + (1 - x)/x}, \quad (24b)$$

and

$$\frac{V_t}{V_{t0}} = \frac{S + \sqrt{\bar{C}_t} f (1 - \alpha)/\alpha}{1 + \sqrt{\bar{C}_t} f (1 - \alpha)/\alpha} \frac{1 + (1 - \alpha)/\alpha}{S + (1 - \alpha)/\alpha} \quad (25a)$$

$$= \frac{S + \sqrt{\bar{C}_t} S (1 - x)/x}{1 + \sqrt{\bar{C}_t} S (1 - x)/x} \frac{f/S + (1 - x)/x}{f + (1 - x)/x}. \quad (25b)$$

The ratio of the void fraction is also derived in the same way:

$$\frac{\alpha}{\alpha_0} (= V_0/V_g) = \frac{1 + (1/S)(1 - \alpha)/\alpha}{1 + (1 - \alpha)/\alpha} \quad (26a)$$

$$= \frac{f + (1 - x)/x}{f + S(1 - x)/x} \quad (26b)$$

Some calculated results of Eqs. (23a) through (26b) are shown in Figs. 4 through 16 with slip and density ratios as parameters. For a drag disk and a turbine meter, \bar{C}_d and \bar{C}_t are taken as unity for lack of other information. This is equivalent to the assumption that the gas and the liquid velocities exert forces in the same manner on the target of a drag disk and on turbine blades.¹⁴

The effects of parameters \bar{C}_d and \bar{C}_t in Eqs. (24a) through (25b) are shown in Figs. 17 through 24.

3.2 Comparison with Homogeneous Model (INEL Method)

For two-phase flow measurement in a pipe during blowdown, the same combination of a gamma densitometer, a drag disk, and a turbine meter has also been used at the Idaho National Engineering Laboratory (INEL). By assuming the flow is homogeneous,¹⁵ even though there may be some slip between two phases, two different mass fluxes (i.e., the mass flux G_d determined by the readings of a densitometer and a drag disk and the mass flux G_t determined by the reading of a densitometer and a turbine meter) were computed and compared with each other. The computed mass fluxes were considered valid when they agreed with each other. There is still some chance, however, that the mass fluxes are incorrect, since both might overestimate or underestimate.

The INEL method is compared with the proposed model as follows.

G_d and G_t are expressed as

$$G_d = \rho_a V_d \quad , \quad (27)$$

and

$$G_t = \rho_a V_t \quad , \quad (28)$$

where V_d is the apparent velocity based on treating the momentum flux measurement of a drag disk in dispersed flow with slip with the homogeneous flow assumption. The relationship between V_d and I_d is expressed by

$$I_d = C_{dg} \alpha \rho_g V_d^2 [1 + \bar{C}_d f (1 - \alpha)/\alpha]$$

[see Eq. (5)]. When $\bar{C}_d = 1$, Eq. (27) corresponds to the expression

$$G_d = \sqrt{\rho_a (I_d / C_{dg})}$$

In a manner similar to that used in the previous section, the ratios of mass fluxes from the INEL method (G_d or G_t) and the proposed model (G) are

$$\frac{G_d}{G} = \frac{1 + f (1 - \alpha)/\alpha}{S + f (1 - \alpha)/\alpha} \sqrt{\frac{S^2 + \bar{C}_d f (1 - \alpha)/\alpha}{1 + \bar{C}_d f (1 - \alpha)/\alpha}} \quad (29a)$$

$$= \frac{(1/S) + (1 - x)/x}{1 + (1 - x)/x} \sqrt{\frac{S + \bar{C}_d (1 - x)/x}{(1/S) + \bar{C}_d (1 - x)/x}} \quad (29b)$$

and

$$\frac{G_t}{G} = \frac{1 + f (1 - \alpha)/\alpha}{S + f (1 - \alpha)/\alpha} \frac{S + \sqrt{\bar{C}_t f (1 - \alpha)/\alpha}}{1 + \sqrt{\bar{C}_t f (1 - \alpha)/\alpha}} \quad (30a)$$

$$= \frac{(1/S) + (1 - x)/x}{1 + (1 - x)/x} \frac{S + \sqrt{\bar{C}_t S (1 - x)/x}}{1 + \sqrt{\bar{C}_t S (1 - x)/x}} \quad (30b)$$

Equations (29b) and (30b) indicate that G_d/G and G_t/G are independent of the density ratio f when the quality x is chosen as a variable. Some calculated results are shown in Figs. 25 through 28, in which \bar{C}_d and \bar{C}_t are assumed equal to 1. The curves of G_t/G have a maximum greater than unity and a minimum less than unity. Comparing Figs. 25 and 27, it is seen that the maximum value of G_t/G is larger than the maximum value of G_d/G at any given slip ratio. The parameter combination in Figs. 25 and 27 are chosen in accordance with the relationship between slip ratio and pressure for steam-water two-phase flow proposed by Thom (Fig. 1). Curves

C in these figures indicate the expected reduction in error if, by some means, the slip ratio is decreased from 5 to 2.

From Fig. 25, it can be said that in dispersed flow the mass flux determined by a densitometer and a drag disk is very close to the real mass flux at low and middle void fractions. Therefore, we can assume that G_d represents the mass flux at a void fraction less than 70 to 80% in dispersed flow. However, the quality of the dispersed flow is quite different from that derived through the homogeneity assumption. For example, if the slip ratio is 2, corresponding to a pressure of about 500 psia for steam-water two-phase flow according to Thom, the real quality is twice that obtained using the homogeneity assumption. This difference has a great influence on the assessment of the enthalpy balance of the system during blowdown. Consequently, the quality or the slip ratio should be measured or calculated by other means.

The effects of parameters \bar{C}_d and \bar{C}_t in Eqs. (29a) through (30b) are indicated in Figs. 29 through 34.

3.3 Comparison with Popper's Model

Popper^{14,16,17} proposed to measure the void fraction of two-phase flow in a pipe with two turbine meters. One is installed upstream, where the flow is single (liquid) phase and measures the local liquid velocity V_{ff} and the other is installed in two-phase flow. From the continuity equations evaluated at the two measuring locations, the void fraction of two-phase flow at the second measuring point is deduced as

$$\alpha = \frac{V_f - V_{ff} (1 - x)}{V_f} , \quad (31)$$

in which the difference of liquid densities at the two locations is ignored. Popper then assumed that the reading of the turbine meter in two-phase flow represents the local liquid velocity when the density of the gas phase is much less than that of the liquid phase. Therefore, the void fraction calculated by Popper's model may be written as

$$\alpha_{CP} = \frac{V_t - V_{ff} (1 - x)}{V_t} . \quad (32)$$

Assuming the relationship between V_f and V_t is expressed by Eq. (16), the relative difference between the proposed model and Popper's model becomes

$$\frac{\alpha_{CP} - \alpha}{\alpha} = \frac{1 - \alpha}{\alpha} \frac{S - 1}{S + \sqrt{\bar{C}_t} f (1 - \alpha)/\alpha} \quad (33)$$

Equation (16) is rewritten as

$$\frac{V_f}{V_t} = \frac{1 + \sqrt{\bar{C}_t} f (1 - \alpha)/\alpha}{S + \sqrt{\bar{C}_t} f (1 - \alpha)/\alpha} \quad (34a)$$

$$= \frac{1 + \sqrt{\bar{C}_t} S (1 - x)/x}{S + \sqrt{\bar{C}_t} S (1 - x)/x} \quad (34b)$$

Figures 35 and 36 show some calculated results of Eq. (34a), and Fig. 37 represents Eq. (34b), which is independent of the density ratio. In these graphs \bar{C}_t is assumed equal to 1.

Figure 38 shows the calculated results of Eq. (33) for steam-water two-phase flow with \bar{C}_t again taken as 1. The combination of slip and density ratios used in this figure are chosen from Fig. 1. Figure 38 shows that the relative difference curves a, b, and c are very close to each other across the rather wide density ratio range from 500 to 12 (equivalent pressure range: 60 to 1500 psia). Both absolute and relative difference curves approach curve d (no difference) as the slip ratio approaches 1. It is interesting to note that relative differences become very large in spite of small absolute differences in void fraction and small errors in measuring the liquid velocity (Figs. 35 to 37) when the void fraction approaches zero. Conversely, relative and absolute differences become very small in spite of probable large errors in measuring liquid velocity (Figs. 35 to 37) when the void fraction approaches unity. Therefore, it may be erroneous to say that at high void fraction the turbine meter measures the liquid velocity when the void fraction calculated by Popper's method corresponds to the void fraction determined with a gamma densitometer.

Figure 39 shows the effect of parameter \bar{C}_t in Eq. (33).

3.4 Comparison with Rouhani's Model

Rouhani^{18,19} proposed another method to calculate void fraction and other quantities characteristic of two-phase flow. The readings of a turbine meter, as well as measured values of mass flow rate, quality, and pressure, were used to compute the void fraction α_{CR} .

In his theory, the modeling of a turbine meter is based on momentum exchange at the turbine blades. The mass fluxes exerting forces on turbine blades are assumed to be AGx and $AG(1-x)$ for steam and water phases, respectively, whereas in the model presented here the fluxes are assumed to be proportional to $\alpha \rho_g (V_g - V_t)$ and $(1-\alpha) \rho_f (V_t - V_f)$ respectively.

The extent of blade overlap defines two extremes in turbine meter design. If the design of turbine blades is like that of Fig. 40a (no overlap), the effective steam mass flux exerting forces on blades seems to be proportional to $\overline{BC/AC}$ (Gx), that is, proportional to $\alpha \rho_g (V_g - V_t)$, and the effective water mass flux seems proportional to $\overline{B'C/AC}$ [$G(1-x)$], that is, $(1-\alpha) \rho_f (V_t - V_f)$. If the design of turbine blades is like that of Fig. 40b, the effective mass fluxes impinging on the blades approach AGx and $AG(1-x)$ for steam and water phases as the overlap increases. Turbine meters to be used in THTF at ORNL are of type (a).

By using Eq. (4) of Ref. 18, the calculated turbine meter velocity V_{tR} and α_{CR} are expressed as

$$V_{tR} = G \left[\frac{x^2}{\alpha \rho_g} + \frac{(1-x)^2}{(1-\alpha) \rho_f} \right] \quad (35)$$

and

$$V_t = G \left[\frac{x^2}{\alpha_{CR} \rho_g} + \frac{(1-x)^2}{(1-\alpha_{CR}) \rho_f} \right]. \quad (36)$$

Assuming again that V_t/V_f is expressed by Eq. (16), the following

relationships are derived:

$$\frac{V_{tR}}{V_t} = \frac{S^2 + f(1-\alpha)/\alpha}{S + f(1-\alpha)/\alpha} \frac{1 + \sqrt{\bar{C}_t f(1-\alpha)/\alpha}}{S + \sqrt{\bar{C}_t f(1-\alpha)/\alpha}} \quad (37a)$$

$$= \frac{S + (1-x)/x}{1 + (1-x)/x} \frac{1 + \sqrt{\bar{C}_t S(1-x)/x}}{S + \sqrt{\bar{C}_t S(1-x)/x}} \quad (37b)$$

and

$$\alpha_{CR} = \frac{1}{2K_1} [(K_1 + K_2 - K_3) + \sqrt{(K_1 + K_2 - K_3)^2 - 4K_1K_2}] \quad , \quad (38)$$

where

$$K_1 = \frac{1}{\alpha} \frac{S + \sqrt{\bar{C}_t f(1-\alpha)/\alpha}}{1 + \sqrt{\bar{C}_t f(1-\alpha)/\alpha}} \quad ,$$

$$K_2 = \frac{S^2}{S + f(1-\alpha)/\alpha} \quad ,$$

and

$$K_3 = \frac{f[(1-\alpha)/\alpha]^2}{S + f(1-\alpha)/\alpha} \quad .$$

Figures 41 to 43 show some calculated results of Eqs. (37a), (37b), and (38) for $\bar{C}_t = 1$. They compare the calculated turbine meter velocities and void fractions of the proposed model and Rouhani's model. The difference between two calculated void fractions at $S = 2$, $f = 50$, and $\bar{C}_t = 1$ (Fig. 43) is less than 5%, nearly the same as that between the new model and Popper's model (Figs. 38 and 39).

4. COMPARISON OF FOUR TURBINE METER MODELS WITH ROUHANI'S DATA

The behavior of a turbine meter seems to be the most uncertain of the three devices discussed here. The experimental data of Rouhani,¹⁹

used for verifying his turbine meter model to measure void fraction or quality in steam-water two-phase flow, can be used to compare the proposed model, Rouhani's model, the homogeneous model, and Popper's model. Calculated void fractions and mass flow rates will be compared with Rouhani's data. Although the Rouhani and Popper models were not originally developed for the measurement of flow rate, they are applied to calculate the flow rate here. The following ranges of variables were covered in Rouhani's experiment.

Pressure	145-725 psia
Mass flux	$0.382 \times 10^6 - 1.36 \times 10^6 \text{ lb}_m/\text{hr}/\text{ft}$
Steam quality	0.0015-0.360
Void fraction	0.010-0.90

In all cases, vertical upflow in a 0.24-in.-ID pipe was examined.

The numerical data consist of 151 sets of pressure, quality, mass flow rate, measured void fraction, and void fraction calculated by his model. The turbine meter velocity is not included; however, it may be calculated using Eq. (36).

4.1 Void Fraction

Rouhani's method for calculating void fraction was discussed in the previous section. Procedures for the other three models are discussed here.

From Eqs. (10a) and (16), the relationship between the void fraction α_{CA} calculated using the proposed model and measured variables is derived as

$$V_t = \frac{G}{\alpha_{CA} \rho_g S + (1 - \alpha_{CA}) \rho_f} \frac{S + \sqrt{\bar{C}_t f (1 - \alpha_{CA}) / \alpha_{CA}}}{1 + \sqrt{\bar{C}_t f (1 - \alpha_{CA}) / \alpha_{CA}}} \quad (39)$$

The void fraction by homogeneous model, α_{ct} , is obtained by inserting

$V_g = V_f = V_t$ in Eq. (10a), that is,

$$\alpha_{Ct} = \frac{\rho_f - (G/V_t)}{\rho_f - \rho_g} \quad (40)$$

Substituting $G = \rho_f V_{ff} A$ in Eq. (32), the void fraction by Popper's method, α_{CP} , is rewritten as

$$\alpha_{CP} = 1 - \frac{G}{\rho_f A V_t} (1 - x) \quad (41)$$

Note that turbine meter velocity V_t is proportional to mass flux G in all four models. Some calculated results of void fraction by the four models are shown in Table 1. The mean error and root-mean-square (rms) errors of void fraction in the table are defined as

$$\text{Mean error} = \frac{\sum (\alpha_C - \alpha)}{N} \quad (42)$$

$$\text{rms error} = \left[\frac{\sum (\alpha_C - \alpha)^2}{N} \right]^{1/2} \quad (43)$$

where N is the number of data and α_C represents α_{CA} , α_{CR} , α_{Ct} , or α_{CP} .

Table 1. Errors in calculated void fraction and mass flux by four models to Rouhani's 151 data^a

	Proposed model, $C_t = 1$	Rouhani's model	Homogeneous model	Popper's model
Void fraction				
Mean error	-0.014	0.012	0.029	0.038
rms error	0.033	0.027	0.038	0.047
Mass flux				
Mean error	-0.018	0.044	0.161	0.251
rms error	0.085	0.081	0.224	0.350

^aThe negative sign indicates an underestimate.

There are no significant differences among the four models, which yield average errors between -1.4 and 3.8%. At $\bar{C}_t = 2.3$, the proposed model gives its lowest rms error of 2.7% and a mean error of 0.1%. These errors are nearly the same as the 2.5% error involved in Rouhani's void-fraction measurement with a (γ, n) void gage.²⁰ Therefore, it is difficult to say which model is the most appropriate for void-fraction measurement in two-phase flow.

4.2 Mass Flow Rate

Calculated mass fluxes by four models are derived from substituting measured void fraction for calculated void fraction in Eqs. (36) and (39) through (41). That is,

$$G_A = [\alpha \rho_g S + (1 - \alpha) \rho_f] \frac{1 + \sqrt{\bar{C}_t f (1 - \alpha)/\alpha}}{S + \sqrt{\bar{C}_t f (1 - \alpha)/\alpha}} V_t , \quad (44)$$

$$G_R = \frac{V_t}{(x^2/\alpha \rho_g) + [(1 - x)^2/(1 - \alpha) \rho_f]} , \quad (45)$$

$$G_t = [\alpha \rho_g + (1 - \alpha) \rho_f] V_t , \quad (46)$$

$$G_P = [\alpha \rho_g S + (1 - \alpha) \rho_f] V_t , \quad (47)$$

for the proposed, Rouhani, homogeneous, and Popper models respectively. A slip ratio in Eqs. (45) and (47) can be calculated through Eq. (8) using measured void fraction, quality, and pressure. G_A is used in this section to distinguish mass flux calculated by the proposed model from measured mass flux G .

Errors of mass flux calculated by four models are shown in Table 2. Mean and rms errors of mass flux are:

$$\text{Mean error} = \frac{\Sigma (G_C - G)/G}{N} , \quad (48)$$

Table 2. Errors of calculated mass flux by four models^a (negative signs are underestimates, $C_t = 1$)

Range of slip ratio	Mean slip ratio	Range of quality	Mean quality	Number of data	Void fraction	Mean void fraction	Mean error $\frac{G_A - G}{G}$	Mean error $\frac{G_R - G}{G}$	Mean relative difference $\frac{(G_R - G_A)/G_A}{G_A}$	Mean error $\frac{G_t - G}{G}$	Mean relative difference $\frac{(G_t - G_A)/G}{G_A}$	Mean error $\frac{G_P - G}{G}$	Mean relative difference $\frac{(G_P - G_A)/G_A}{G_A}$
0.8-1.2	1.007	0.01-0.05	0.028	7	0.45-0.59	0.532	0.014	0.015	0.001	0.016	0.001	0.016	0.001
1.5-2.0	1.730	0.01-0.05	0.033	14	0.35-0.64	0.479	-0.054	0.005	0.064	0.015	0.075	0.030	0.090
	1.776	0.05-0.10	0.071	10	0.54-0.83	0.667	-0.009	0.063	0.074	0.086	0.098	0.121	0.133
	1.888	0.10-0.15	0.119	4	0.72-0.74	0.730	0.072	0.151	0.074	0.202	0.121	0.273	0.187
	1.917	0.15-0.20	0.176	1	0.78	0.778	0.069	0.132	0.059	0.204	0.126	0.315	0.230
2.0-2.5	2.156	0.01-0.05	0.027	6	0.28-0.66	0.481	-0.084	-0.010	0.084	0.006	0.101	0.021	0.117
	2.162	0.05-0.10	0.077	9	0.58-0.74	0.656	-0.075	0.010	0.093	0.055	0.141	0.101	0.190
	2.319	0.10-0.15	0.124	10	0.68-0.80	0.729	-0.020	0.061	0.084	0.148	0.172	0.236	0.261
	2.291	0.15-0.20	0.167	3	0.77-0.79	0.781	0.032	0.098	0.065	0.209	0.173	0.334	0.295
2.5-3.0	2.638	0.01-0.05	0.030	7	0.30-0.62	0.485	-0.112	-0.021	0.106	0.008	0.139	0.028	0.161
	2.735	0.05-0.10	0.070	5	0.64-0.76	0.698	-0.044	0.062	0.112	0.137	0.191	0.190	0.247
	2.671	0.10-0.15	0.115	5	0.72-0.81	0.762	0.032	0.127	0.092	0.246	0.208	0.343	0.302
	2.719	0.15-0.20	0.167	6	0.74-0.82	0.776	-0.024	0.037	0.062	0.193	0.223	0.334	0.367
	2.759	0.20-0.25	0.223	5	0.80-0.87	0.826	0.042	0.070	0.026	0.277	0.226	0.489	0.429
3.0-3.5	3.279	0.01-0.05	0.027	4	0.32-0.68	0.534	-0.108	-0.002	0.123	0.041	0.170	0.061	0.192
	3.291	0.05-0.10	0.093	1	0.73	0.730	-0.059	0.042	0.108	0.182	0.257	0.265	0.344
	3.273	0.10-0.15	0.123	2	0.75-0.82	0.783	0.004	0.091	0.086	0.274	0.271	0.392	0.389
	3.212	0.15-0.20	0.179	2	0.84-0.87	0.853	0.077	0.124	0.044	0.376	0.278	0.570	0.457
	3.339	0.20-0.25	0.210	1	0.87	0.873	0.131	0.149	0.015	0.462	0.292	0.714	0.515
3.5-4.5	3.518	0.01-0.05	0.033	2	0.62-0.64	0.633	-0.098	0.021	0.132	0.081	0.198	0.107	0.227
	4.037	0.05-0.10	0.080	2	0.75-0.82	0.785	-0.052	0.057	0.118	0.237	0.305	0.317	0.388
	3.817	0.10-0.15	0.135	4	0.77-0.86	0.805	-0.007	0.060	0.068	0.318	0.327	0.463	0.473
	3.937	0.15-0.20	0.172	2	0.81-0.83	0.819	0.005	0.034	0.029	0.357	0.350	0.557	0.549
4.5-5.5	4.508	0.01-0.05	0.047	2	0.65-0.66	0.657	-0.121	0.005	0.144	0.128	0.283	0.171	0.332
	4.845	0.05-0.10	0.080	6	0.67-0.79	0.752	-0.073	0.029	0.113	0.262	0.361	0.348	0.453
	5.149	0.10-0.15	0.114	2	0.81-0.82	0.814	-0.039	0.022	0.063	0.367	0.423	0.505	0.566
	5.261	0.15-0.20	0.153	1	0.86	0.857	0.031	0.040	0.009	0.504	0.459	0.716	0.665
5.5-6.5	5.567	0.10-0.15	0.125	3	0.79-0.84	0.815	-0.032	0.006	0.039	0.416	0.463	0.577	0.630
	6.309	0.15-0.20	0.171	2	0.84-0.86	0.850	0.009	-0.041	-0.049	0.565	0.552	0.829	0.812

^a Errors were calculated by Eqs. (37b), (30b), and (34b) using mean values of slip ratio and quality.

$$\text{rms error} = \left[\frac{\sum [(G_C - G)/G]^2}{N} \right]^{1/2}, \quad (49)$$

where N is the number of data and G_C represents G_A , G_R , G_t , or G_P .

There are remarkable differences among four models. The proposed model and Rouhani's model give rms errors that are nearly the same, but the mean error of the former is less than that of the latter. Both the mean and rms errors of the homogeneous model are worse, and those of Popper's model are the worst of all.

Figure 44 shows how accurately the proposed model with $\bar{C}_t = 1$ can predict the mass flow rates measured by Rouhani.

To compare the proposed model with the other models, we can use any equation in the previous sections. Thus, G_t/G_A and G_P/G_A are expressed by Eqs. (30b) and (34b), respectively, and G_R/G_A is derived from Eqs. (35) and (45); that is,

$$\frac{G_R}{G_A} = \frac{V_{tA}}{V_{tR}}, \quad (50)$$

which is the inverse of Eq. (37b). The quantities $(G_R - G_A)/G_A$, $(G_t - G_A)/G_A$, and $(G_P - G_A)/G_A$ calculated through the above equations can be regarded as a measure of difference between the proposed model and the earlier models.

Table 2 presents detailed results of the calculation, and is read in the following manner (1st row):

Seven data points of Rouhani's experiment have slip ratios between 0.8 and 1.2 and qualities between 0.01 and 0.05. The average slip ratio and quality are, respectively, 1.007 and 0.028. Void fraction ranges from 0.45 to 0.59, with an average of 0.532.

Values of $(G_C - G)/G$ for the four models were calculated by Eqs. (37b), (30b), and (34b) as discussed above. Slip ratio and quality were chosen as independent variables for Table 2, so that pressure and void fraction would be eliminated from the three equations for calculating $(G_C - G_A)/G_A$.

The normalized differences $(G_C - G)/G$ of the four flow models for slip ratios in the ranges of 1.5–2.0, 2.0–2.5, 2.5–3.0, and 3.0–3.5 are plotted in Fig. 45 to demonstrate the differences between models. From Fig. 45 and Table 2, it is obvious that for $S > 1$,

$$G_A < G_R < G_t < G_P, \quad (51)$$

with a few exceptions. As seen in Fig. 42, $G_A < G_R$ for qualities below 20 to 30%, $G_A < G_t$ for all but very high qualities (Figs. 28, 33, 34), and $G_A < G_P$ at any quality (Fig. 37).

Though Rouhani's test data contain a few points where $G_A > G_R$ (see the bottom line of Table 2), it does not contain any data at such high qualities that $G_A > G_t$ might occur.

At slip ratios between 0.8 and 1.2, errors of the four models are very low (<1.6%), as expected. At slip ratios between 1.5 and 5.5 and qualities below 5%, Rouhani's method gives the best prediction of flow rate, the proposed model underestimates the flow by 5 to 12%, and the homogeneous model and Popper's method overestimate the flow by up to 13 and 17% respectively. When the slip ratio is between 5.5 and 6.5, the last two models overestimate flows by more than 40%, even at qualities below 5%. At any constant slip ratio, all models have a tendency to overestimate the flow with increasing quality, with the exception of Rouhani's model at a high slip ratio. At qualities more than 20% and slip ratios greater than 3, errors of the homogeneous model and Popper's method become very large (more than 35%).

From the above discussion and Fig. 44, it appears that the proposed model can be used to predict mass flow rates of the Rouhani experiment (nonartificially dispersed flow) with an error of $\pm 10\%$.

The following discussion is suggested to explain why the proposed model underestimates the flow at low qualities and overestimates at higher qualities. At low qualities and void fractions greater than $\sim 30\%$, annular flow may exist. In this case water hits the outer part of the turbine blade, and the liquid velocity influences the turbine more than expected by the new model. As V_f is generally less than V_g , the actual turbine velocity is less than expected. At higher qualities the flow

upstream of a turbine meter may be dispersed, but water droplets may be concentrated around the thick hub of the turbine meter due to their greater inertia relative to that of steam. In this case the steam quality is greatest around the outer regions of the turbine blades, and the steam velocity V_g influences the turbine meter velocity more than expected by the proposed model.

As seen in Table 3, \bar{C}_t has little influence on the void fraction and mass flux calculated with the proposed model.

Table 3. Effect of \bar{C}_t on calculated void fraction and mass using the proposed model with the Rouhani data

\bar{C}_t	0.5	1.0	2.0	3.0
Void fraction				
Mean error	-0.030	-0.014	-0.0003	0.006
rms error	0.045	0.033	0.028	0.028
Mass flux				
Mean error	-0.075	-0.018	0.035	0.063
rms error	0.109	0.085	0.105	0.129

5. CONSIDERATIONS IN THE USE OF THIS MODEL

The proposed model has not been checked with experimental data from an artificially dispersed flow system; however, the comparisons with the Rouhani data are promising, and it is expected that the model accuracy will be increased in a well-dispersed flow.

In addition to sufficient flow dispersal, transient analysis may require the following:

1. The densitometer, drag disk, and turbine meter should be installed as close together as possible, without causing mutual interaction.
2. Response time constants of the three instruments should be the same. If this is not possible, high-frequency filters should be used so that the response time constants of the final data are approximately the same.

In steady or slowly changing flow, these points may be unimportant; however, time lags due to the spacing between devices may be significant in rapid transients and should be minimized. A drag disk usually has a much smaller time constant than a turbine meter. If mass flow is calculated with the proposed model and raw data are not treated with high-frequency filters, the errors might be large, and, in the worst case, b in Eq. (18) might not be defined ($b^2 < 0$).

6. CONCLUSION

Although the proposed model was developed for use in a system with artificially dispersed flow, it yields a good prediction of mass flow rate in nonartificially dispersed flow up to 35% quality with an error of $\pm 10\%$ (much better than that of the homogeneous flow model). The model is intended to be applied over a wider range of conditions than covered by the Rouhani data but needs to be verified over this wider range.

The use of Thom's correlation of slip ratio vs pressure may incur very large errors because of the large scatter of slip ratios at a given pressure.

There is some probability that G_t and G_d based on homogeneous flow do not represent the real mass flux, even when $G_t = G_d$. Based on the evaluation of Rouhani's data G_t overestimates the true value for $S > 1$, and G_d is always expected to do the same.

The proposed model should be a valuable method to compute mass flow rate, quality, slip, and other variables in both steady-state and transient two-phase flows.

ACKNOWLEDGMENT

The author acknowledges the benefit derived from discussions with R. F. Bennett during the preparation of this report. He is also indebted to C. G. Lawson for his kind analysis direction and to D. G. Thomas for his careful critical review.

NOMENCLATURE

A	Cross-section area of a pipe
A_g	Part of cross section occupied by gas phase
\bar{C}_d	Ratio of drag coefficients of a drag disk (C_{df}/C_{dg})
C_{df}	Drag coefficient of a drag disk for liquid phase
C_{dg}	Drag coefficient of a drag disk for gas phase
\bar{C}_t	Ratio of drag coefficient of a turbine blade (C_{tf}/C_{tg})
C_{tf}	Drag coefficient of a turbine blade for liquid phase
C_{tg}	Drag coefficient of a turbine blade for gas phase
D_i	Inside diameter of a pipe
f	Ratio of liquid and gas densities (ρ_f/ρ_g)
G	Mass flow rate per unit area
G_A	Mass flow rate per unit area calculated by the proposed model
G_C	Representative of G_A , G_P , G_R , and G_t
G_d	Mass flow rate per unit area calculated by homogeneous model using the readings of a densitometer and a drag disk
G_P	Mass flow rate per unit area calculated by Popper's method
G_R	Mass flow rate per unit area calculated by Rouhani's method
G_t	Mass flow rate per unit area calculated by the homogeneous model using the readings of a densitometer and a turbine meter
I_d	Momentum flux measured by a drag disk for dispersed flow
I_{d0}	Momentum flux measured by a drag disk in homogeneous flow
m_f	Mass flow rate of liquid phase
m_g	Mass flow rate of gas phase
r	Distance from the axis of a turbine meter
S	Ratio of the gas phase velocity and the liquid phase velocity (V_g/V_f), called the slip ratio

V_d	Imaginary velocity based on the homogeneity assumption for the momentum flux measurement by a drag disk
V_f	Liquid phase velocity in dispersed flow
V_{ff}	Liquid single-phase velocity
V_g	Gas phase velocity in dispersed flow
V_0	Flow velocity in homogeneous flow
V_r	Turning speed of a point on the turbine blade
V_t	Velocity measured by a turbine meter in dispersed flow
V_{t0}	Velocity measured by a turbine meter in homogeneous flow
V_{tR}	Turbine meter velocity calculated by Rouhani's method
W	Mass flow rate in a pipe
x	Gas quality (by weight) defined in Eq. (2)
Y	Dimensionless parameter $[f(1-\alpha)/\alpha]$
α	Void fraction in dispersed flow
α_C	Representative of α_{CA} , α_{CP} , α_{CR} , and α_{Ct}
α_{CA}	Void fraction calculated by the proposed model
α_{CP}	Void fraction calculated by Popper's method
α_{CR}	Void fraction calculated by Rouhani's method
α_{Ct}	Void fraction calculated by the homogeneous model
α_0	Void fraction in homogeneous flow
ρ_{a0}	Apparent density measured by a gamma densitometer in homogeneous flow
ρ_f	Liquid phase density
ρ_g	Gas phase density
ϕ	Twisting angle of a turbine blade (Fig. 3)
ω	Angular velocity of a turbine blade

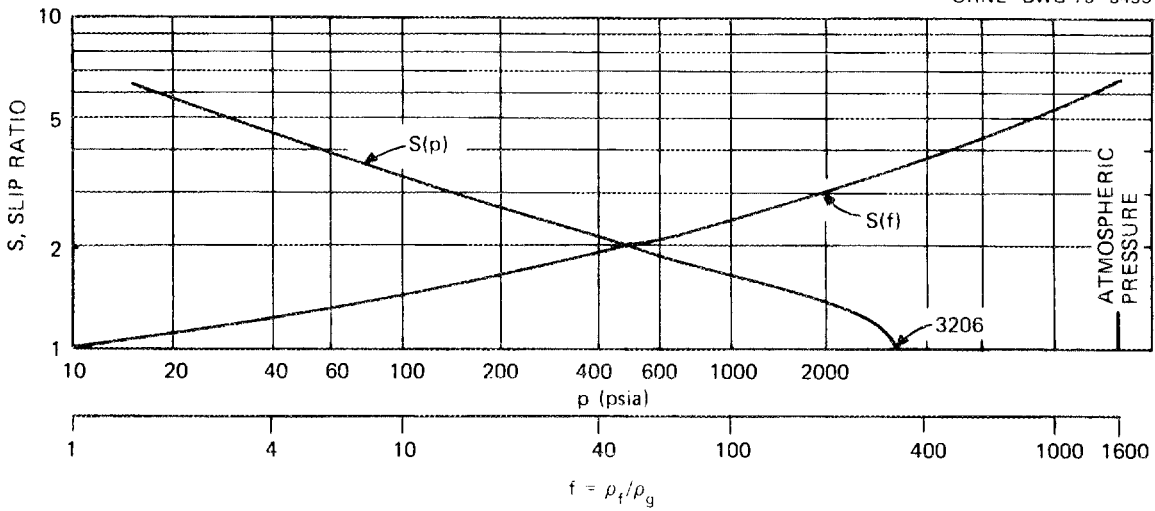


Fig. 1. Slip ratio (V_g/V_f) determined experimentally for steam and water.⁷

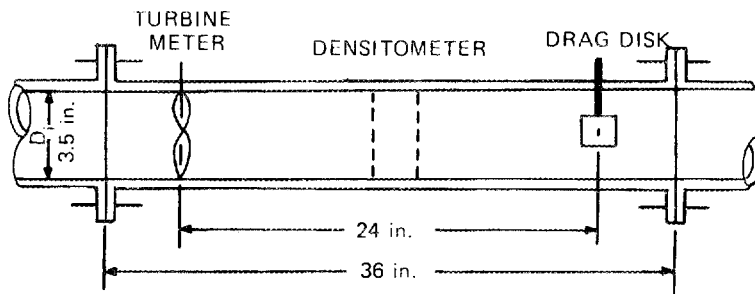


Fig. 2. Arrangement of turbine meter, densitometer, and drag disk in an instrument spool piece of the THTF.

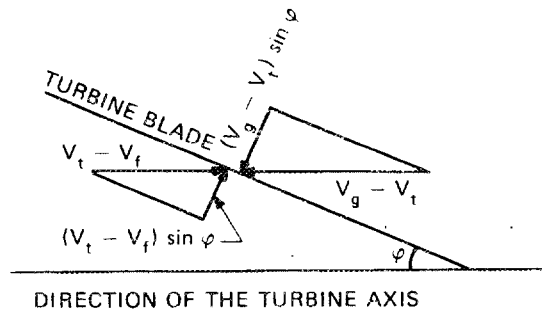


Fig. 3. Velocities of gas and liquid phases relative to turbine blade velocity.

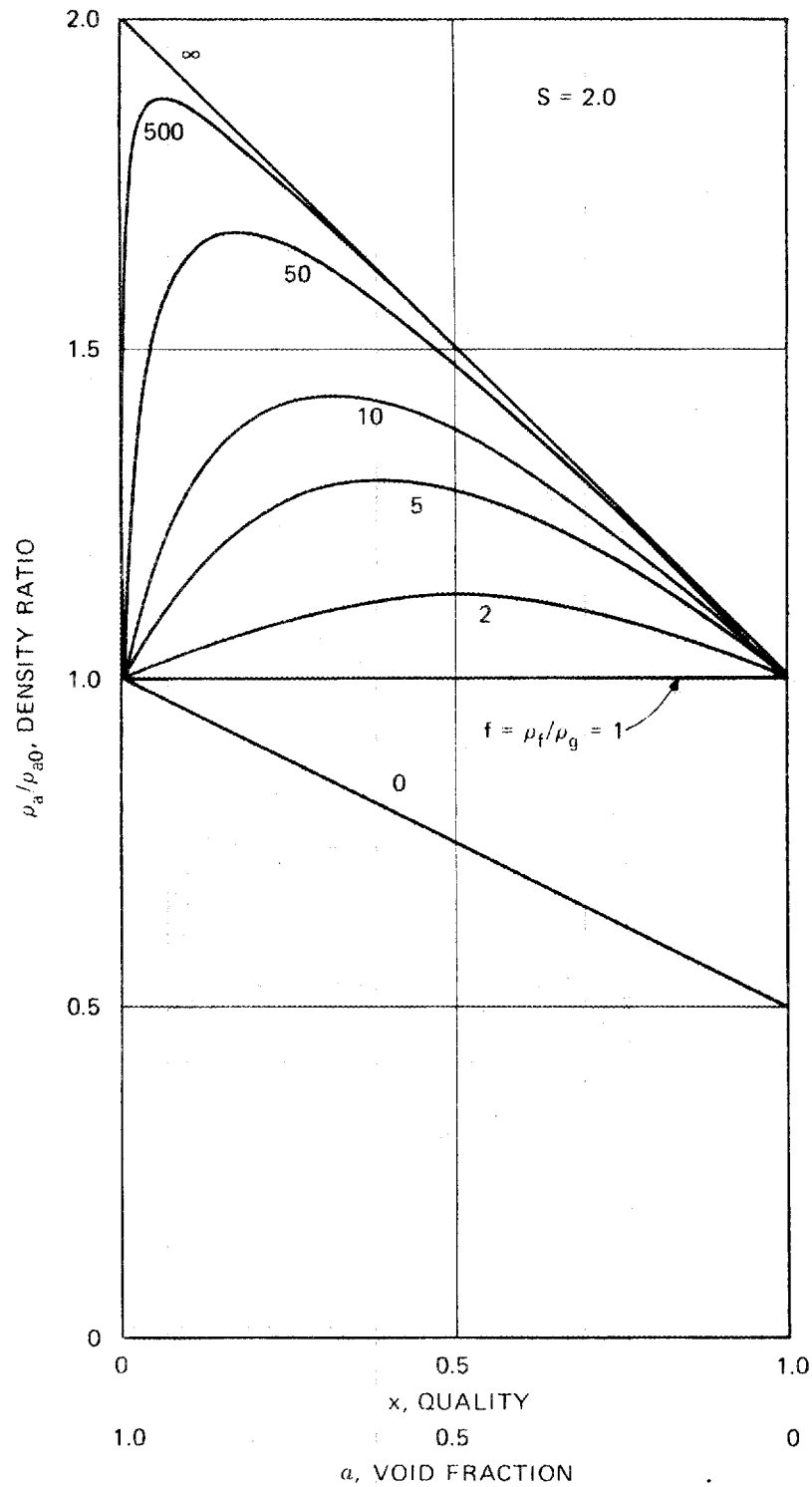


Fig. 4. Influence of phase density ratio on the ratio of apparent densities calculated through the proposed model (ρ_a) and the homogeneous model (ρ_{a0}) for $S = 2.0$ [Eqs. (23a and 23b)].

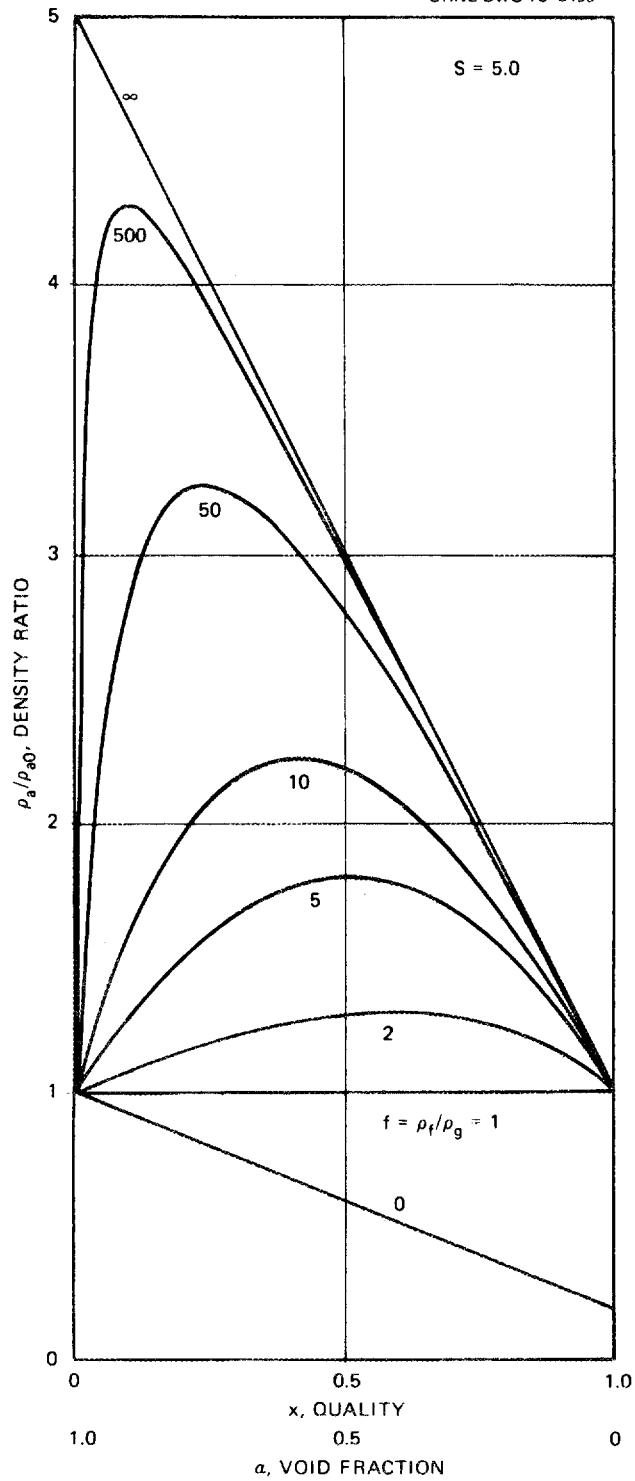


Fig. 5. Influence of phase density ratio on the ratio of apparent densities calculated through the proposed model (ρ_a) and the homogeneous model (ρ_{a0}) for $S = 5.0$ [Eqs. (23a and 23b)].

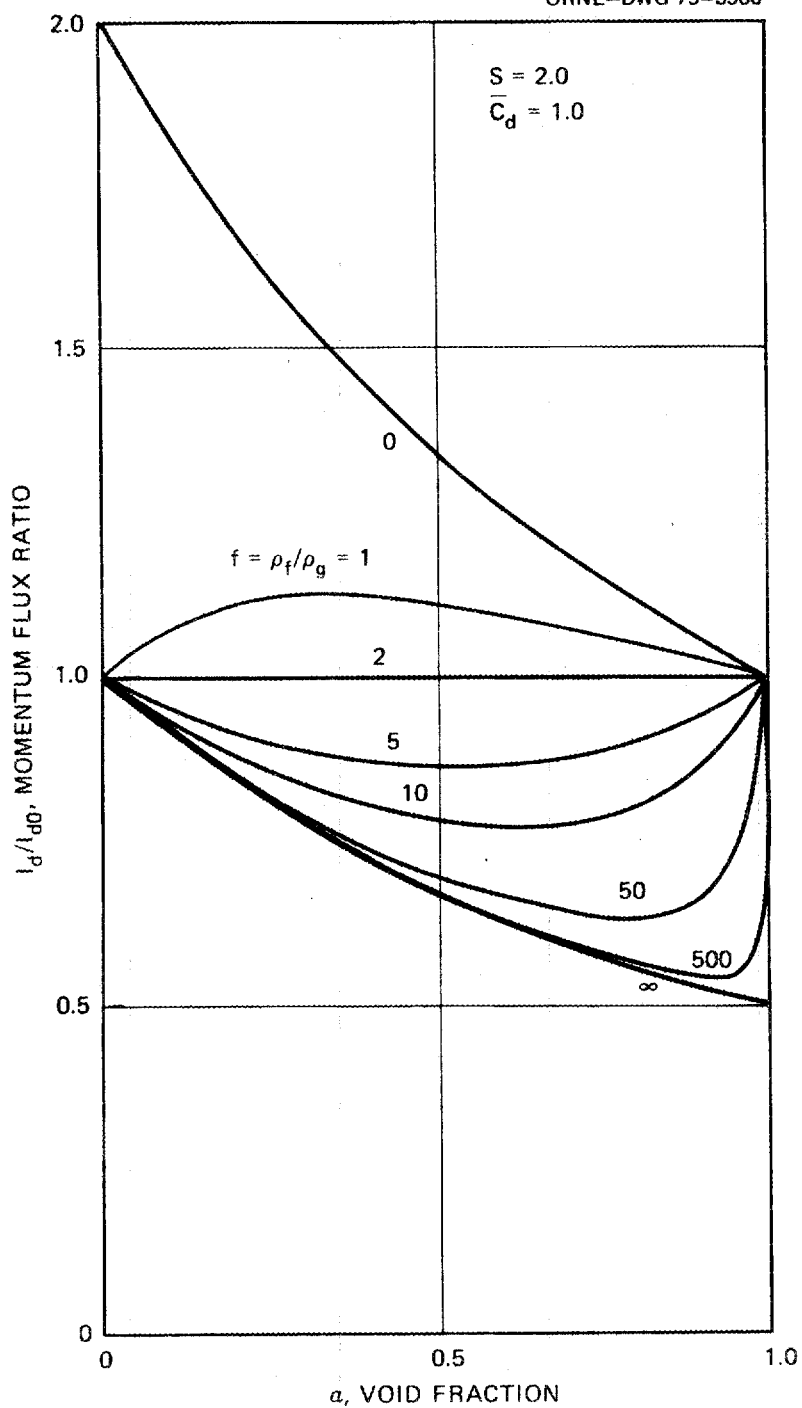


Fig. 6. Influence of phase density ratio on the ratio of momentum fluxes calculated through the proposed model (I_d) and the homogeneous model (I_{d0}) for $S = 2.0$ [Eq. (24a)].

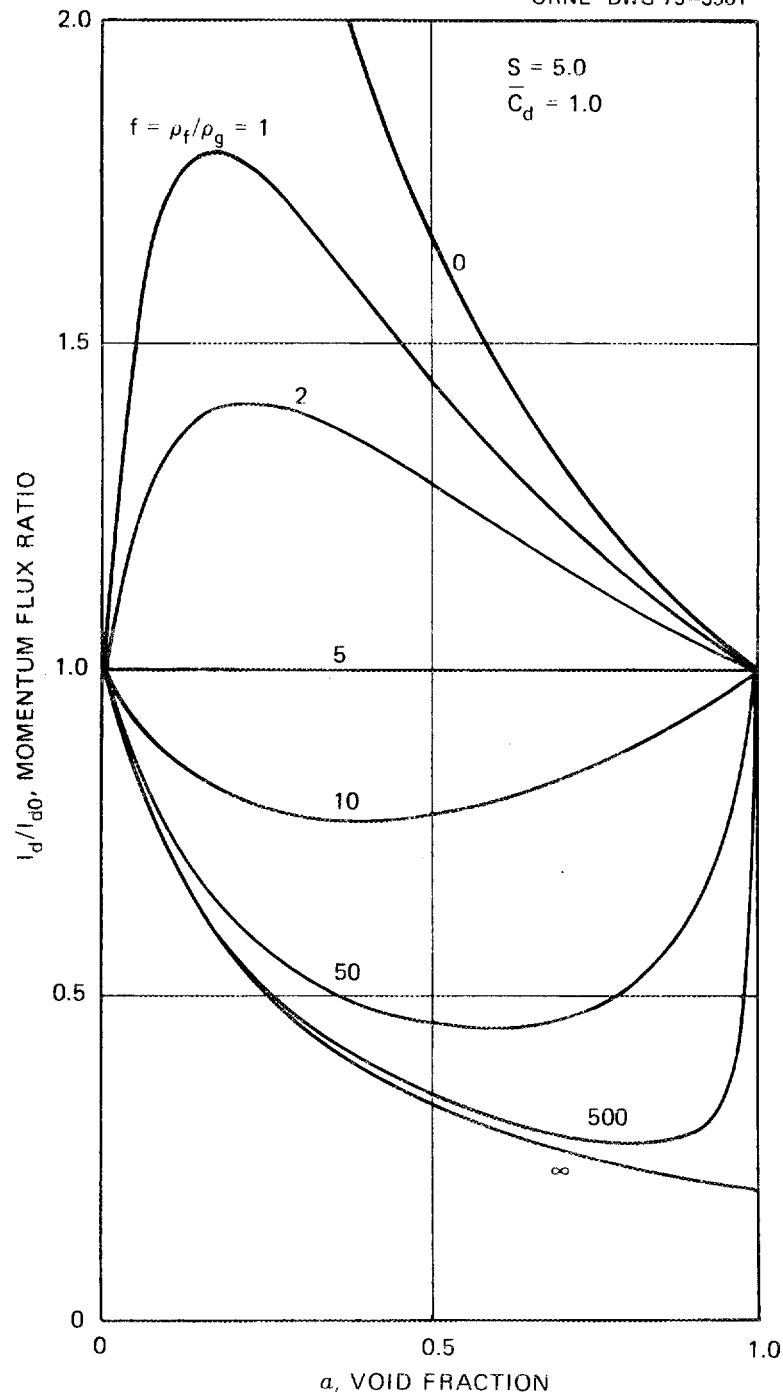


Fig. 7. Influence of phase density ratio on the ratio of momentum fluxes calculated through the proposed model (I_d) and the homogeneous model (I_{d0}) for $S = 5.0$ [Eq. (24a)].

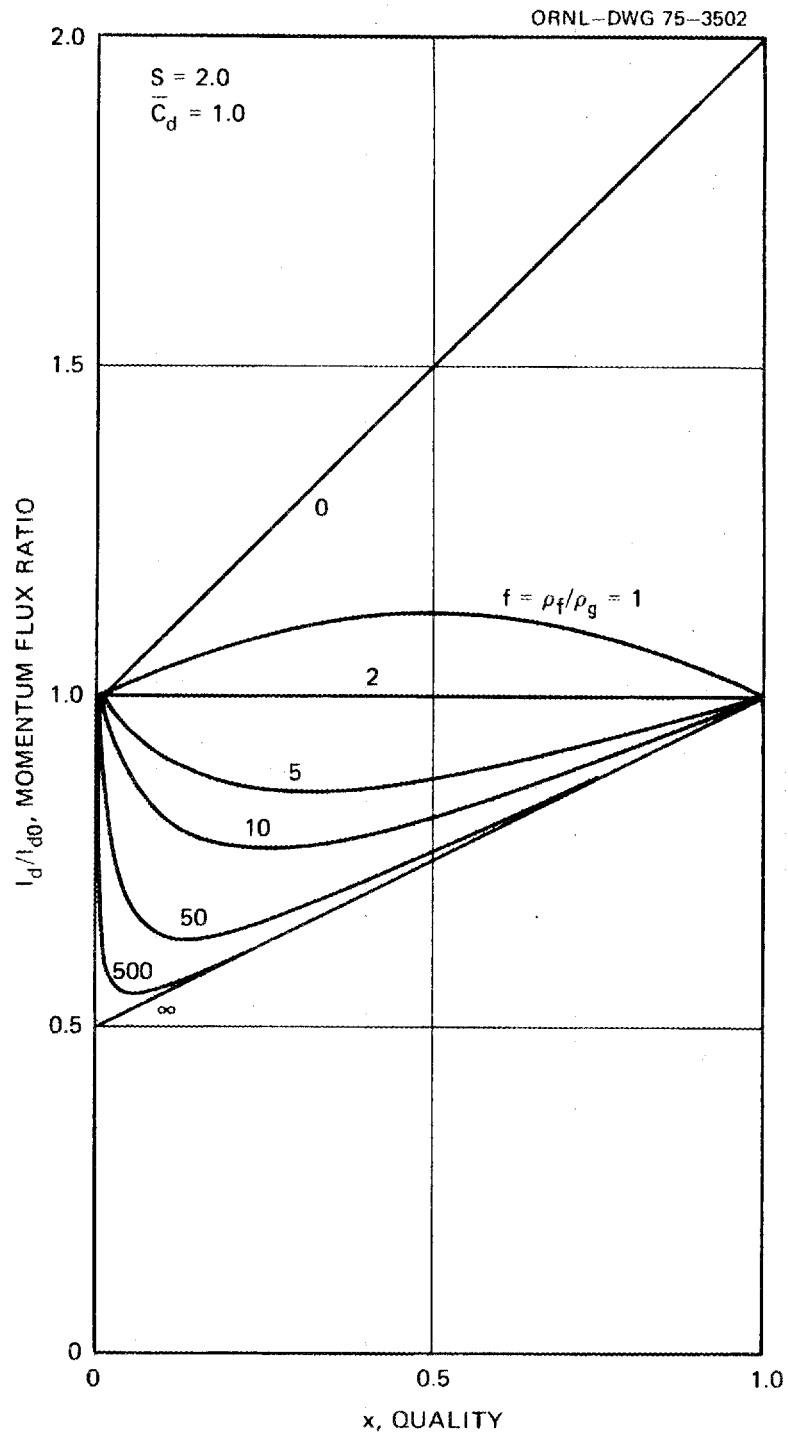


Fig. 8. Influence of phase density ratio on the ratio of momentum fluxes calculated through the proposed model (I_d) and the homogeneous model (I_{d0}) for $S = 2.0$ [Eq. (24b)].

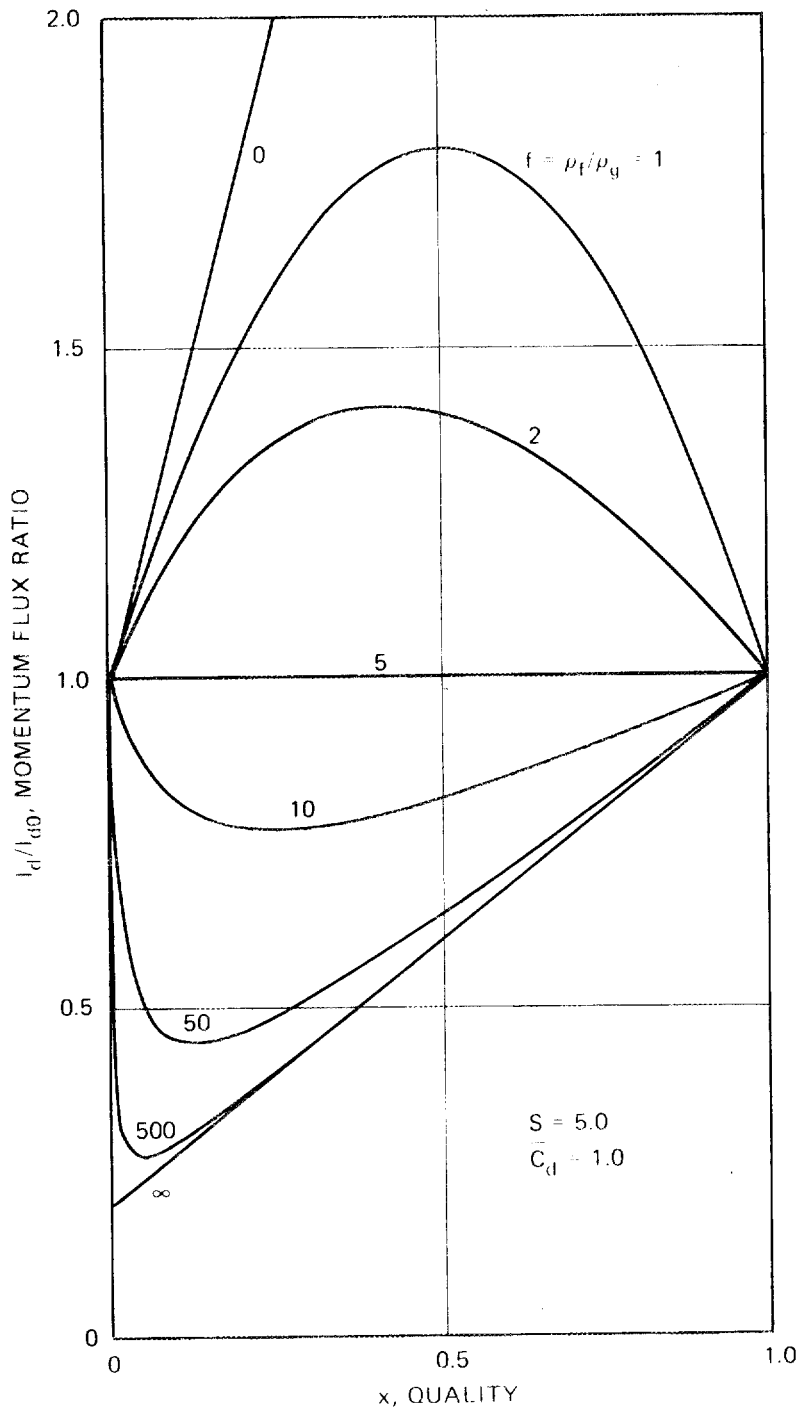


Fig. 9. Influence of phase density ratio on the ratio of momentum fluxes calculated through the proposed model (I_d) and the homogeneous model (I_{d0}) for $S = 5.0$ [Eq. (24b)].

ORNL-DWG 75-3504

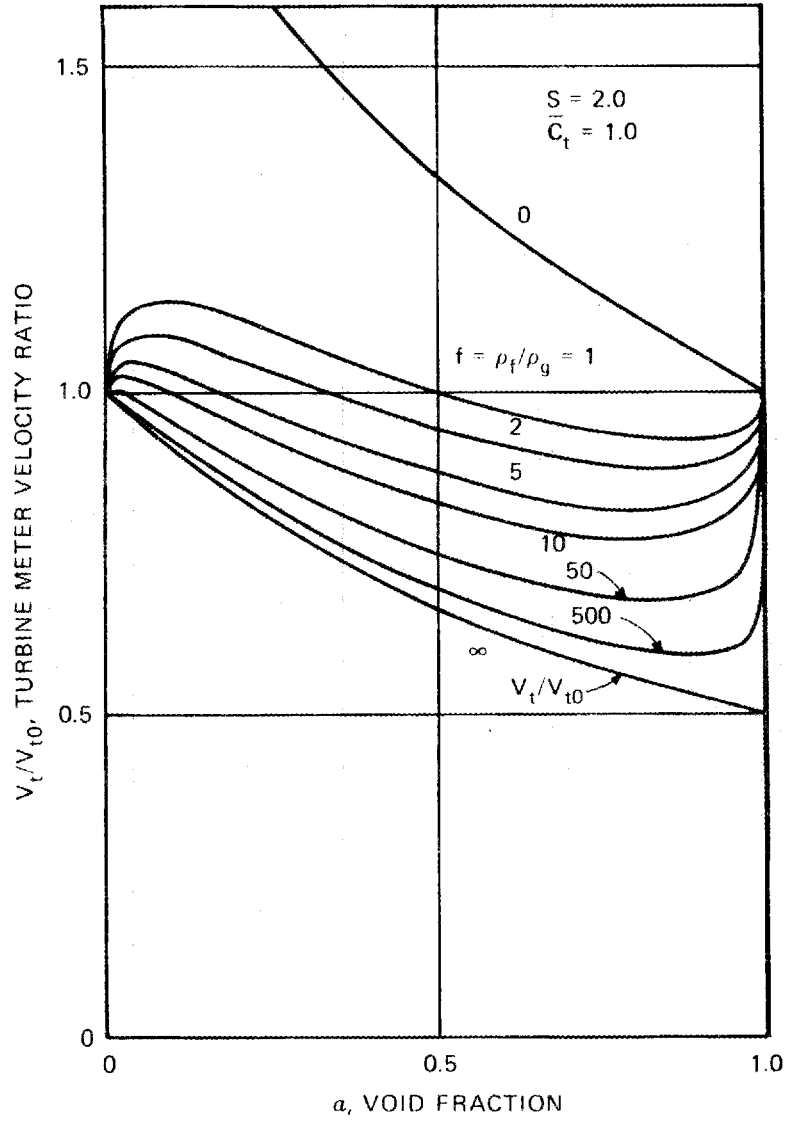


Fig. 10. Influence of phase density ratio on the ratio of turbine meter velocities calculated through the proposed model (V_t) and the homogeneous model (V_{t0}) for $S = 2.0$ [Eq. (25a)].

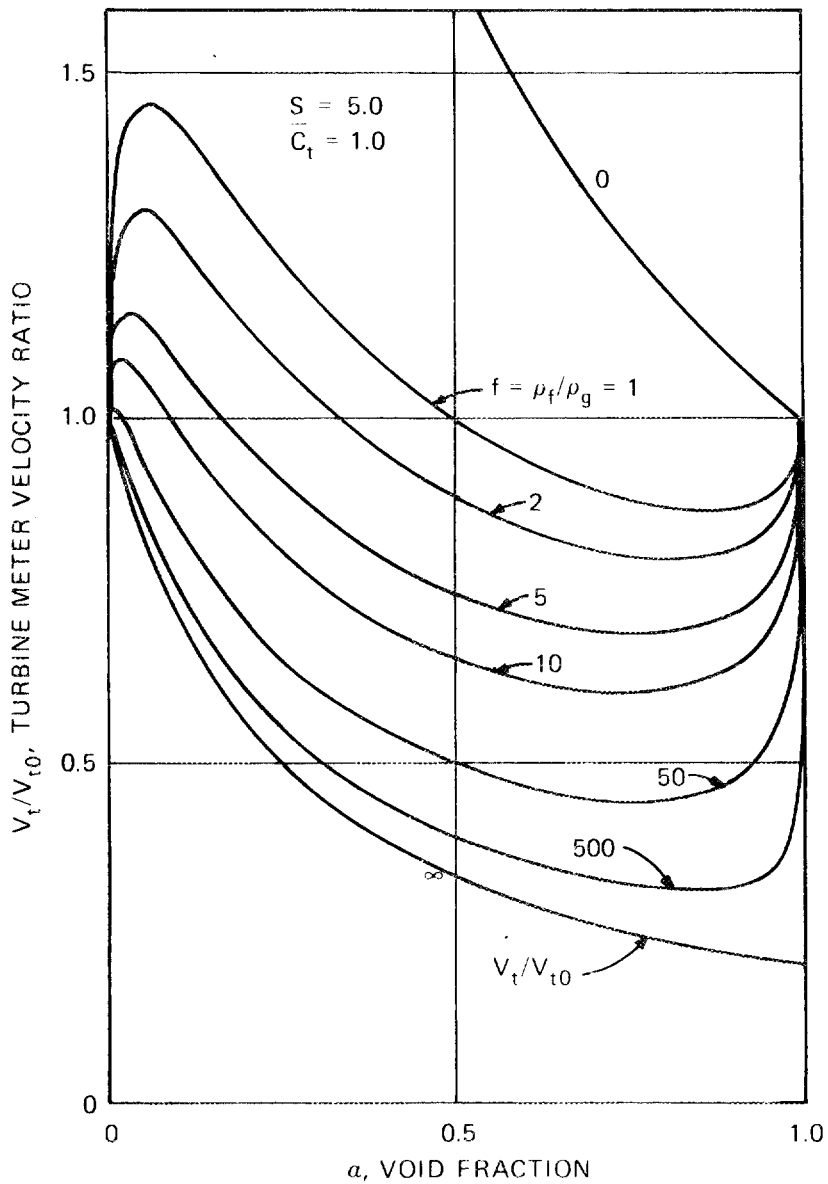


Fig. 11. Influence of phase density ratio on the ratio of turbine meter velocities calculated through the proposed model (V_t) and the homogeneous model (V_{t0}) for $S = 5.0$ [Eq. (25a)].

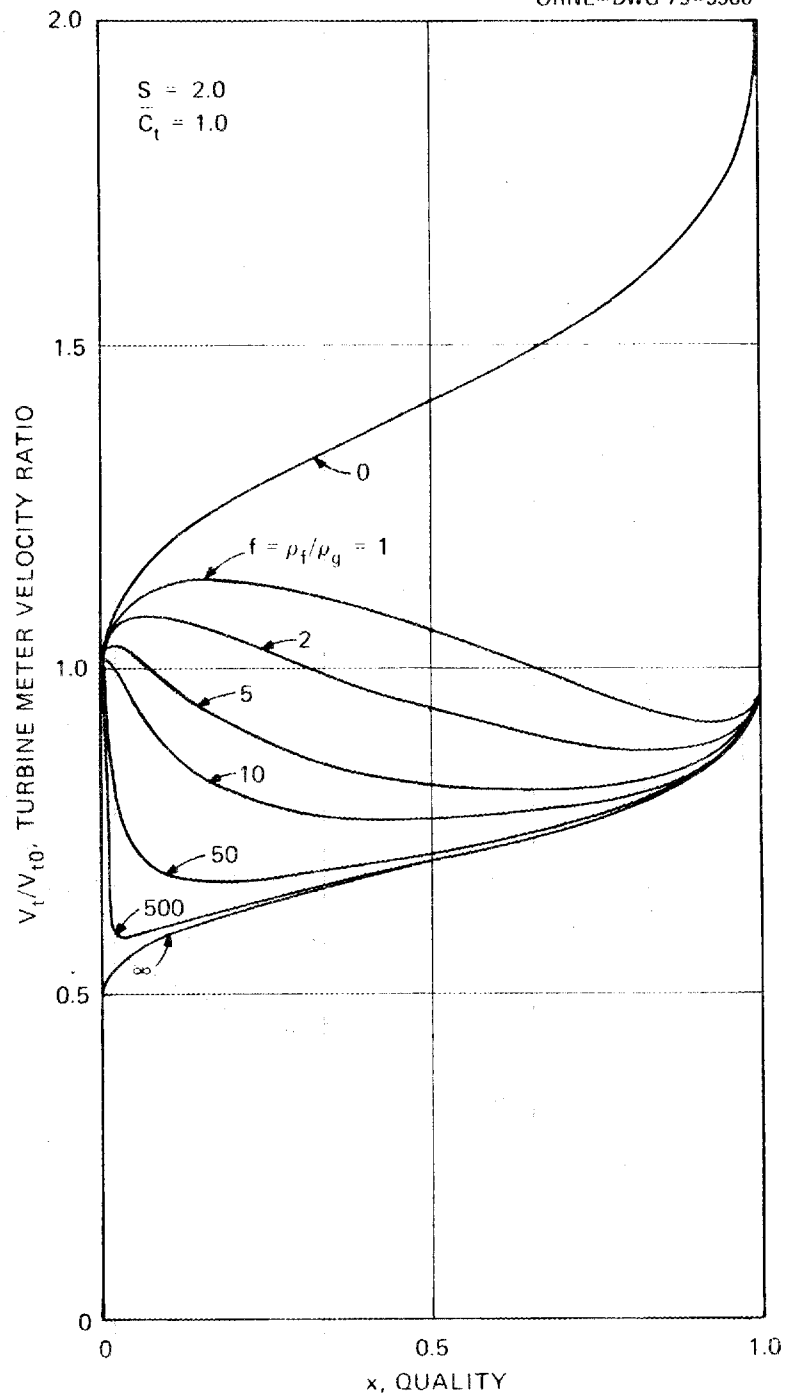


Fig. 12. Influence of phase density ratio on the ratio of turbine meter velocities calculated through the proposed model (V_t) and the homogeneous model (V_{t0}) for $S = 2.0$ [Eq. (25b)].

ORNL-DWG 75-3507

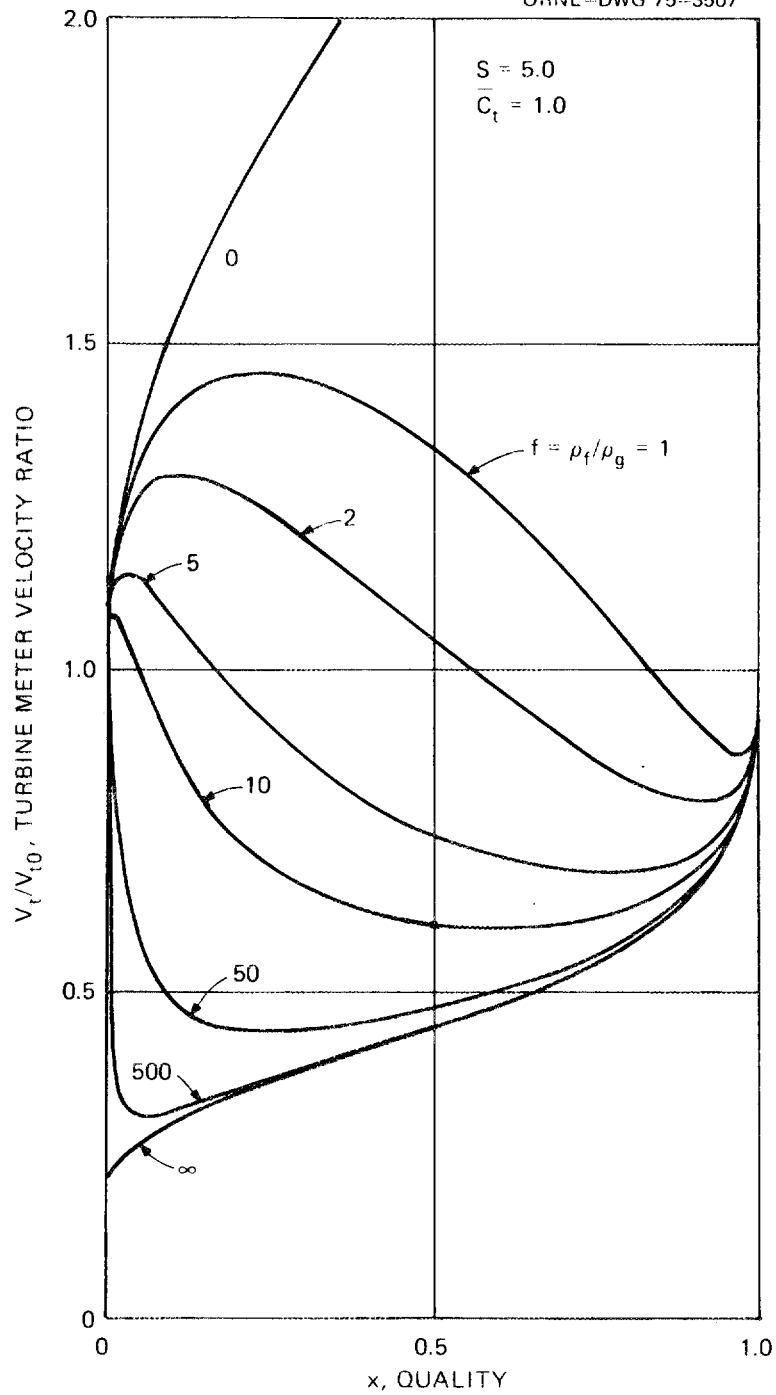


Fig. 13. Influence of phase density ratio on the ratio of turbine meter velocities calculated through the proposed model (V_t) and the homogeneous model (V_{t0}) for $S = 5.0$ [Eq. (25b)].

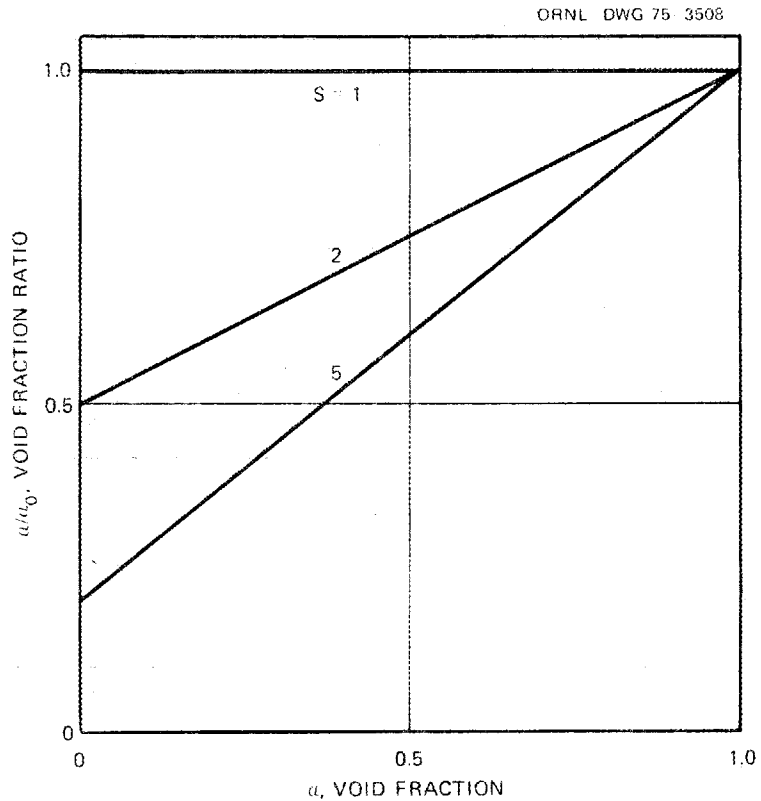


Fig. 14. Ratio of dispersed flow void fraction (α) to homogeneous void fraction (α_0) plotted against dispersed flow void fraction for different slip ratios. In this case the phase volumetric flow rates are important, and the phase density ratio is of no consequence [Eq. (26a)].

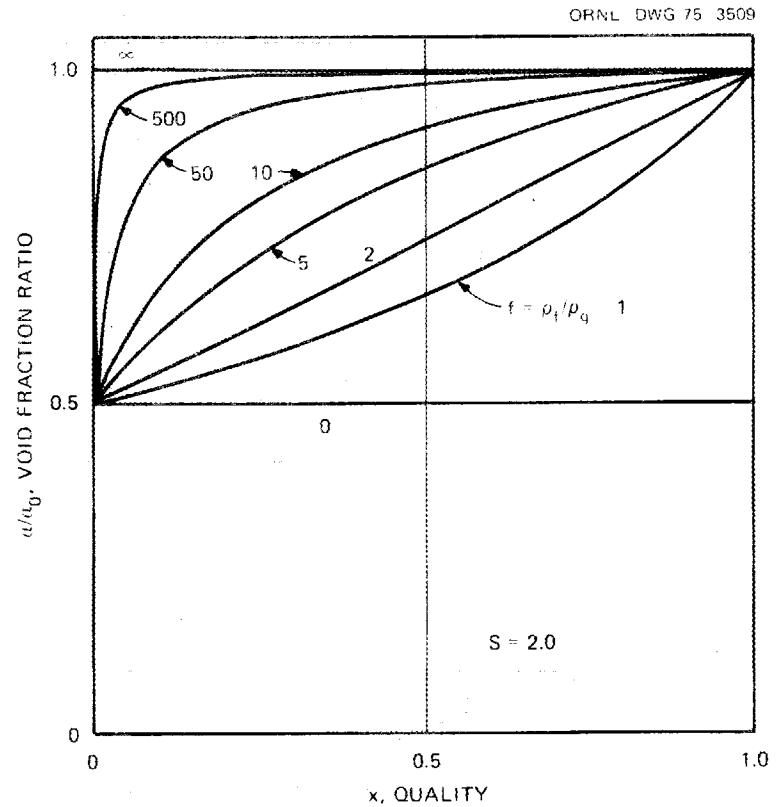


Fig. 15. Ratio of dispersed flow void fraction (α) to homogeneous void fraction (α_0) as a function of quality for different phase density ratios at $S = 2.0$ [Eq. (26b)].

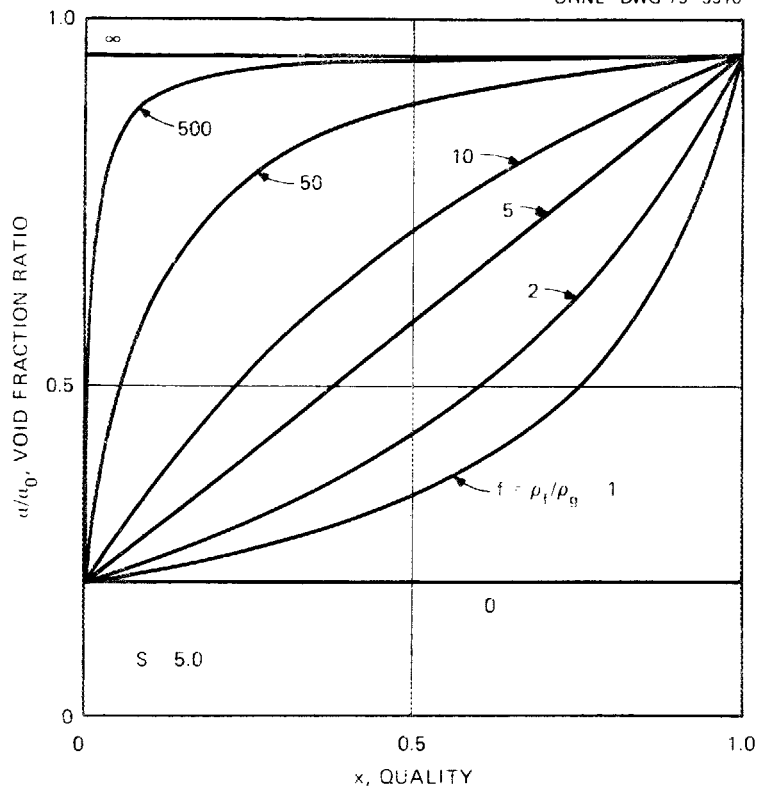


Fig. 16. Ratio of dispersed flow void fraction (α) to homogeneous void fraction (α_0) as a function of quality for different phase density ratios at $S = 5.0$ [Eq. (26b)].

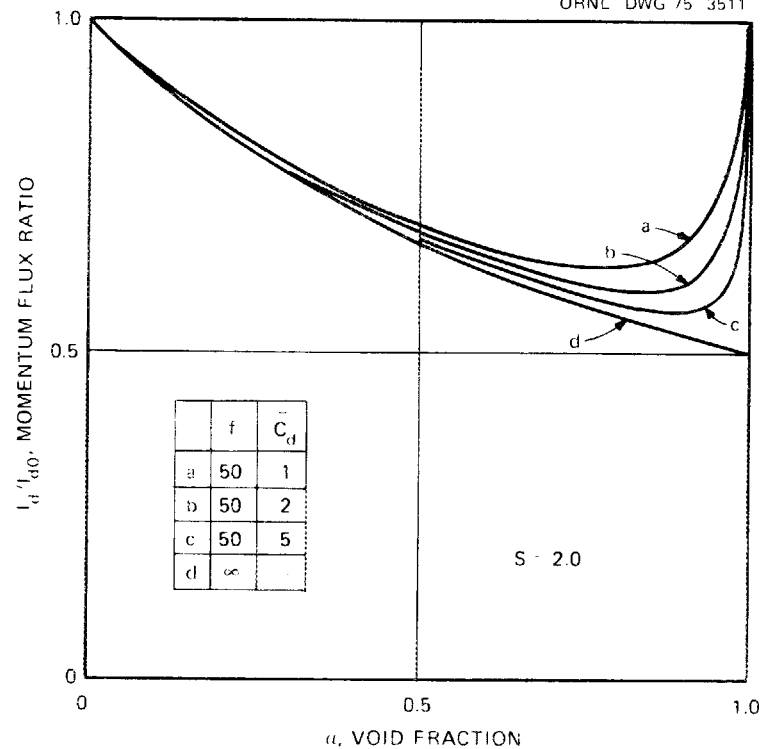


Fig. 17. Influence of \bar{C}_d on the ratio of momentum fluxes calculated through the proposed model (I_d) and the homogeneous model (I_{d0}) for $S = 2.0$ [Eq. (24a)].

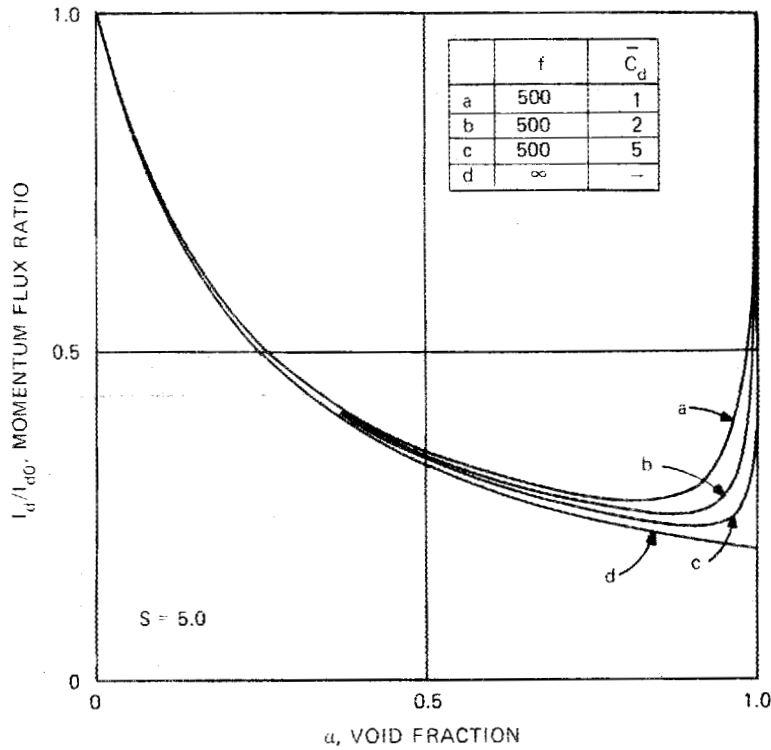


Fig. 18. Influence of \bar{C}_d on the ratio of momentum fluxes calculated through the proposed model (I_d) and the homogeneous model (I_{d0}) for $S = 5.0$ [Eq. (24a)].

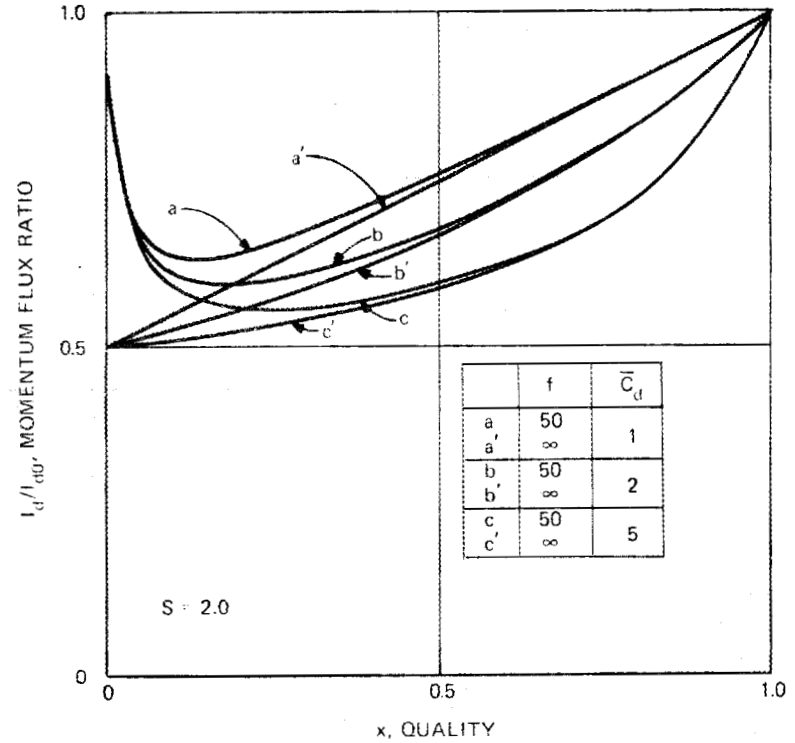


Fig. 19. Influence of \bar{C}_d on the ratio of momentum fluxes calculated through the proposed model (I_d) and the homogeneous model (I_{d0}) for $S = 2.0$ [Eq. (24b)].

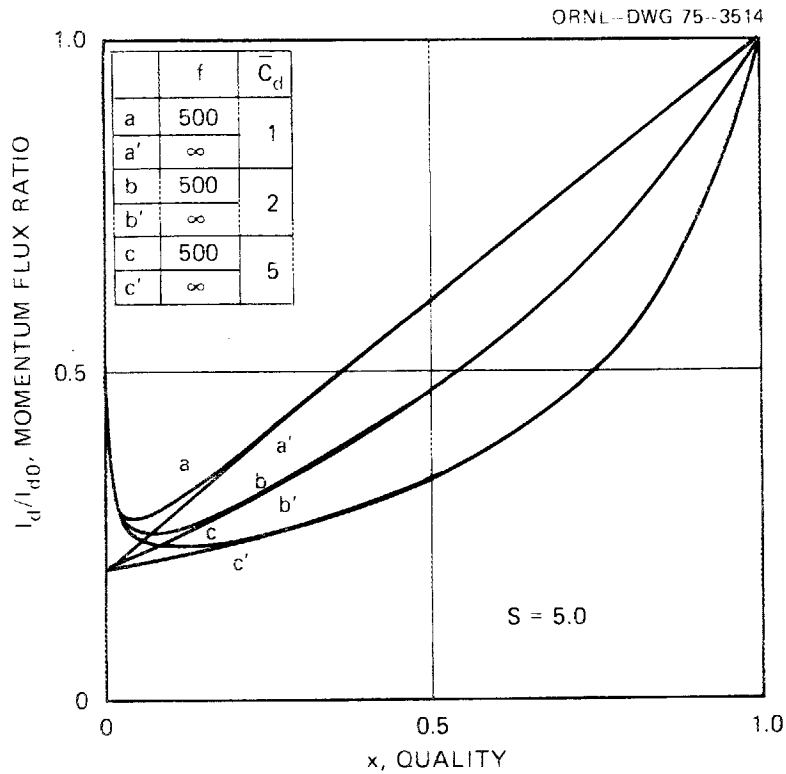


Fig. 20. Influence of \bar{C}_d on the ratio of momentum fluxes calculated through the proposed model (I_d) and the homogeneous model (I_{d0}) for $S = 5.0$ [Eq. (24b)].

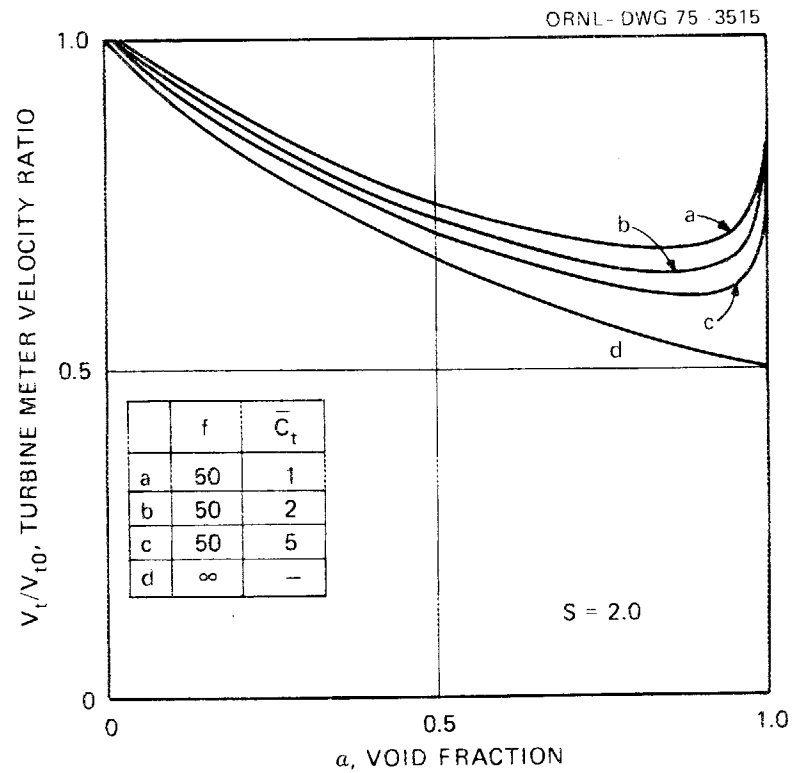


Fig. 21. Influence of \bar{C}_t on the ratio of turbine meter velocities calculated through the proposed model (V_t) and the homogeneous model (V_{t0}) for $S = 2.0$ [Eq. (25a)].

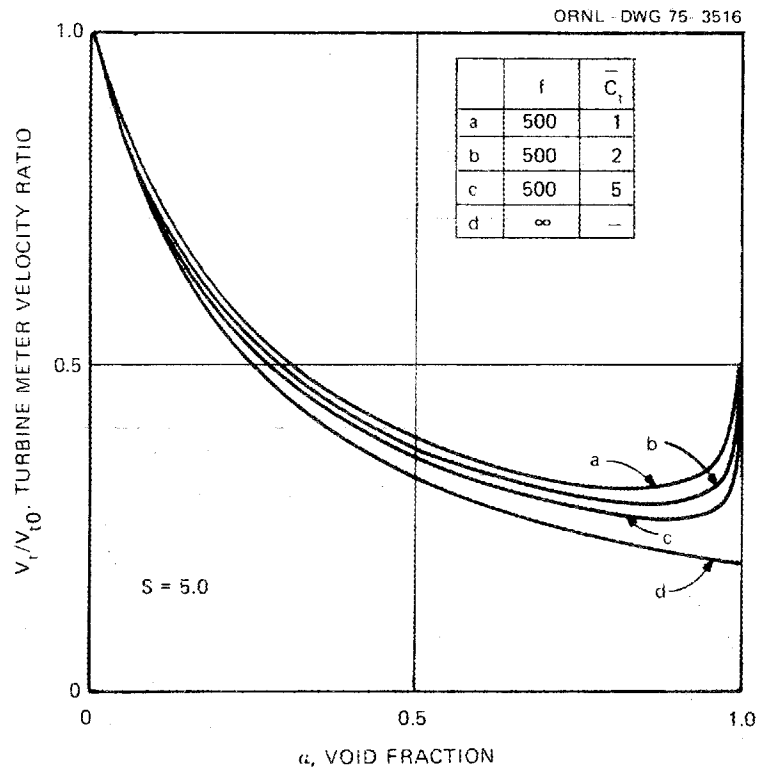


Fig. 22. Influence of \bar{C}_t on the ratio of turbine meter velocities calculated through the proposed model (V_t) and the homogeneous model (V_{t0}) for $S = 5.0$ [Eq. (25a)].

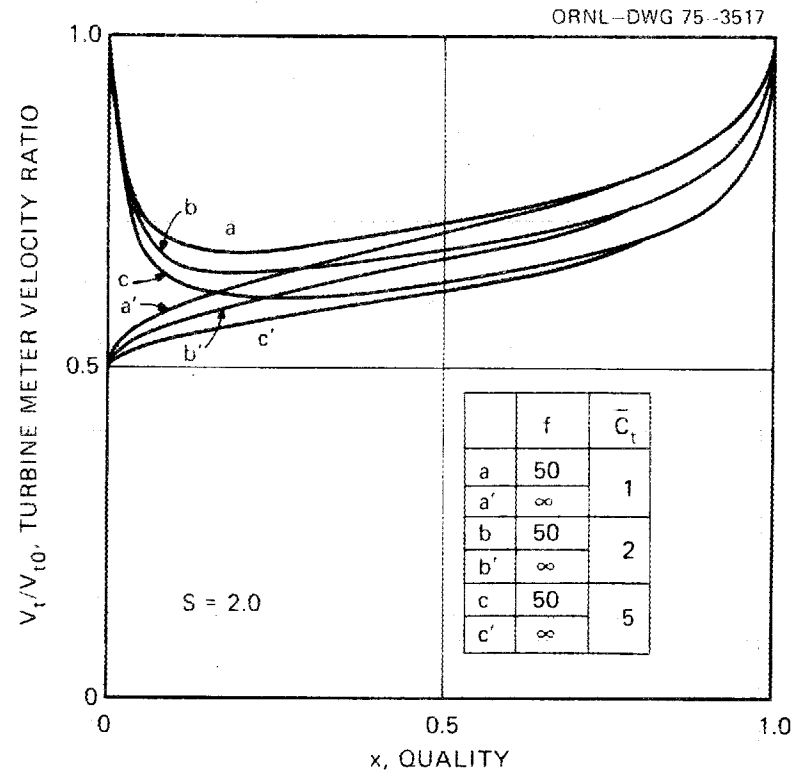


Fig. 23. Influence of \bar{C}_t on the ratio of turbine meter velocities calculated through the proposed model (V_t) and the homogeneous model (V_{t0}) for $S = 2.0$ [Eq. (25b)].

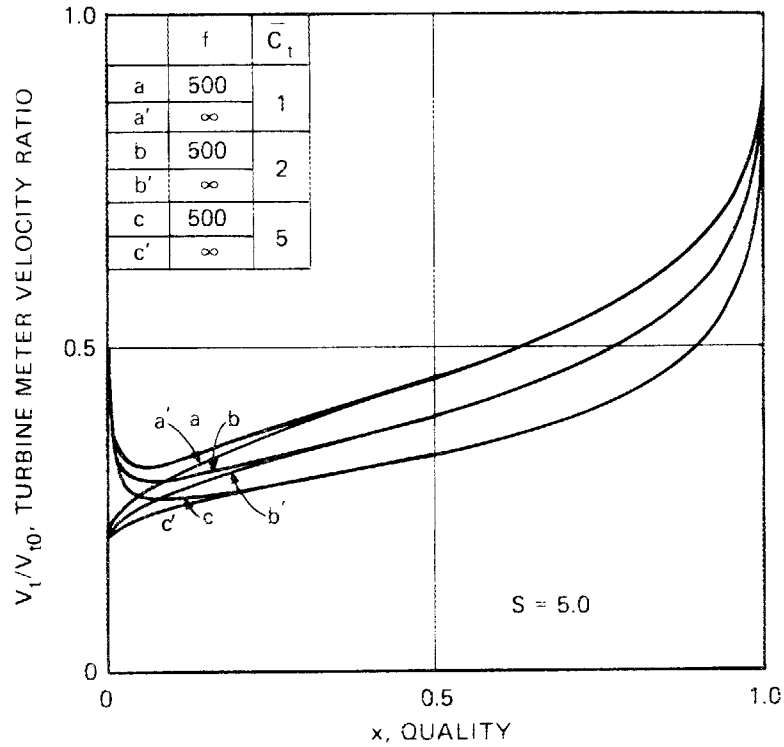


Fig. 24. Influence of \bar{C}_t on the ratio of turbine meter velocities calculated through the proposed model (V_t) and the homogeneous model (V_{t0}) for $S = 5.0$ [Eq. (25b)].

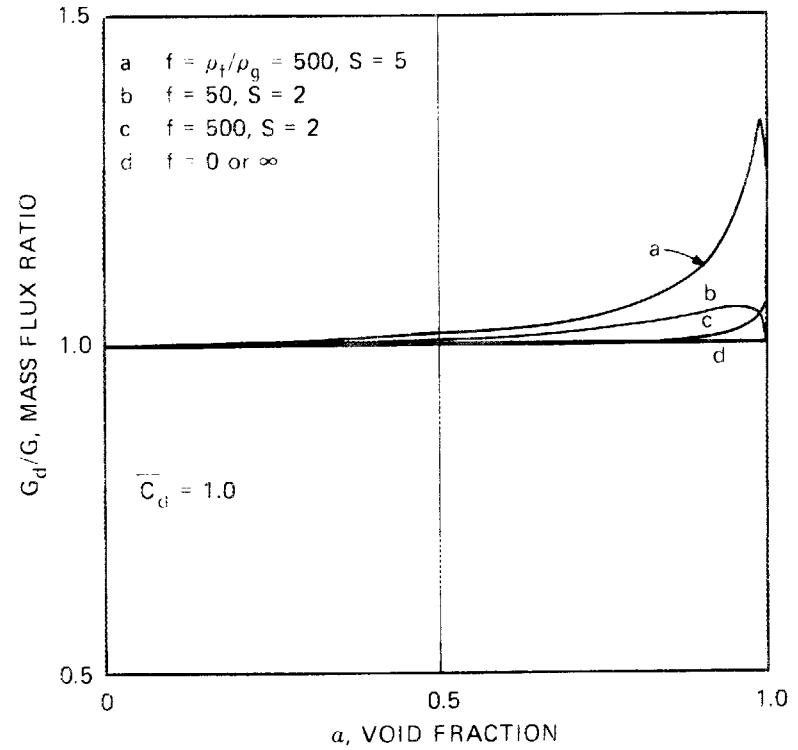


Fig. 25. Ratio of mass fluxes based on INEL method using drag disk and densitometer (G_d) and proposed model (G) vs void fraction for selected values of f and S [Eq. (29a)] and $\bar{C}_d = 1.0$.

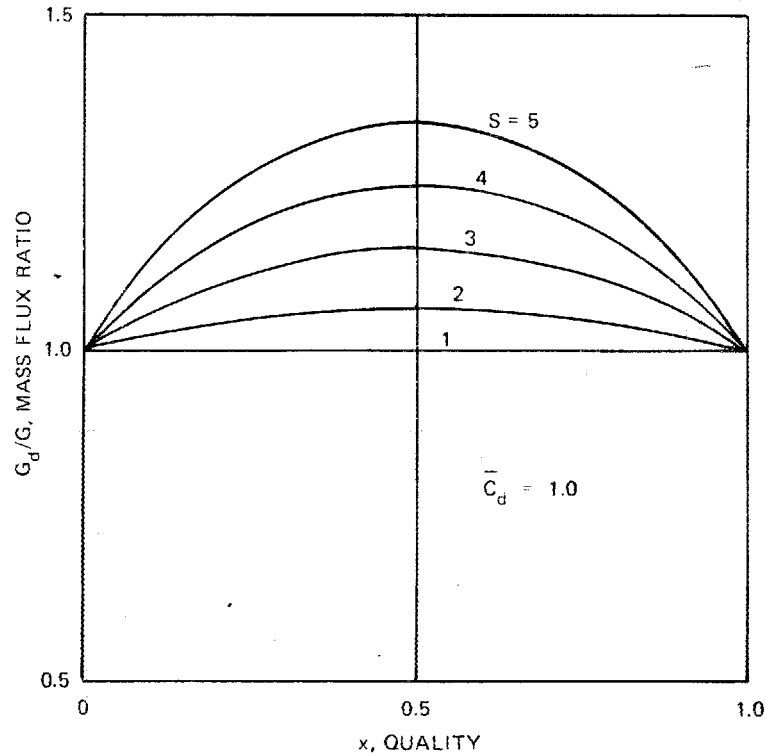


Fig. 26. Ratio of mass fluxes based on INEL method using drag disk and densitometer (G_d) and proposed model (G) vs quality for selected values of S . Use of quality as a parameter eliminates the density ratio f in the expression for G_d/G [Eq. (29b)] and $\bar{C}_d = 1.0$.

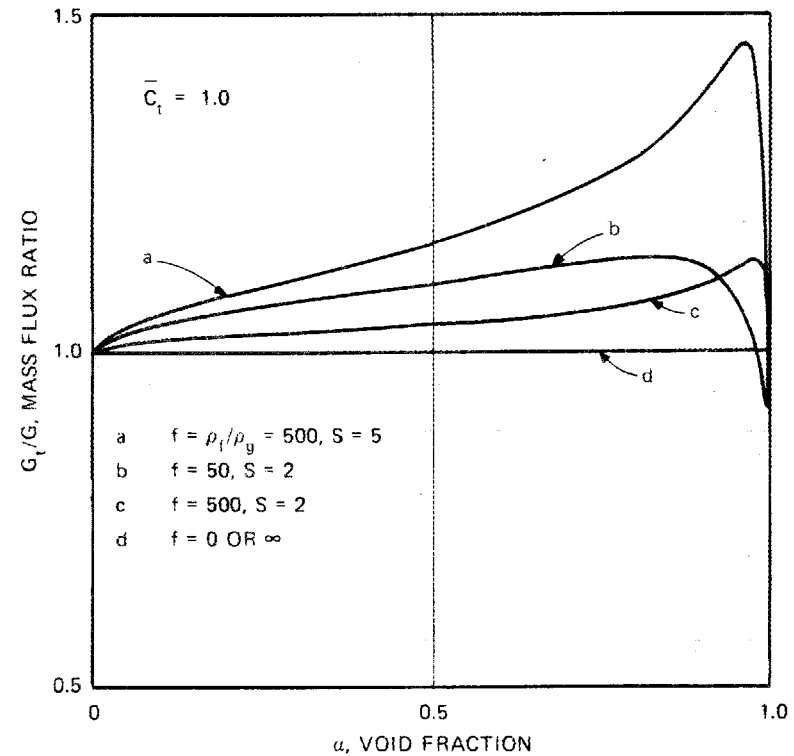


Fig. 27. Ratio of mass fluxes based on INEL method using turbine meter and densitometer (G_t) and proposed model (G) vs void fraction for selected values of f and S [Eq. (30a)] and $\bar{C}_t = 1.0$.

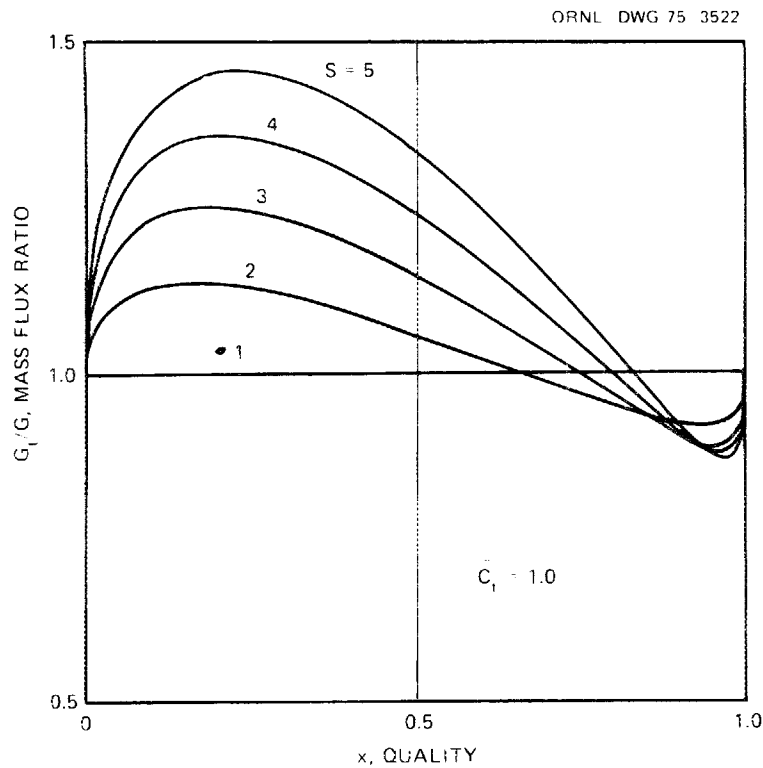


Fig. 28. Ratio of mass fluxes based on INEL method using turbine meter and densitometer (G_t) and proposed model (G) vs quality for selected values of S [Eq. (30b)] and $\bar{C}_t = 1.0$.

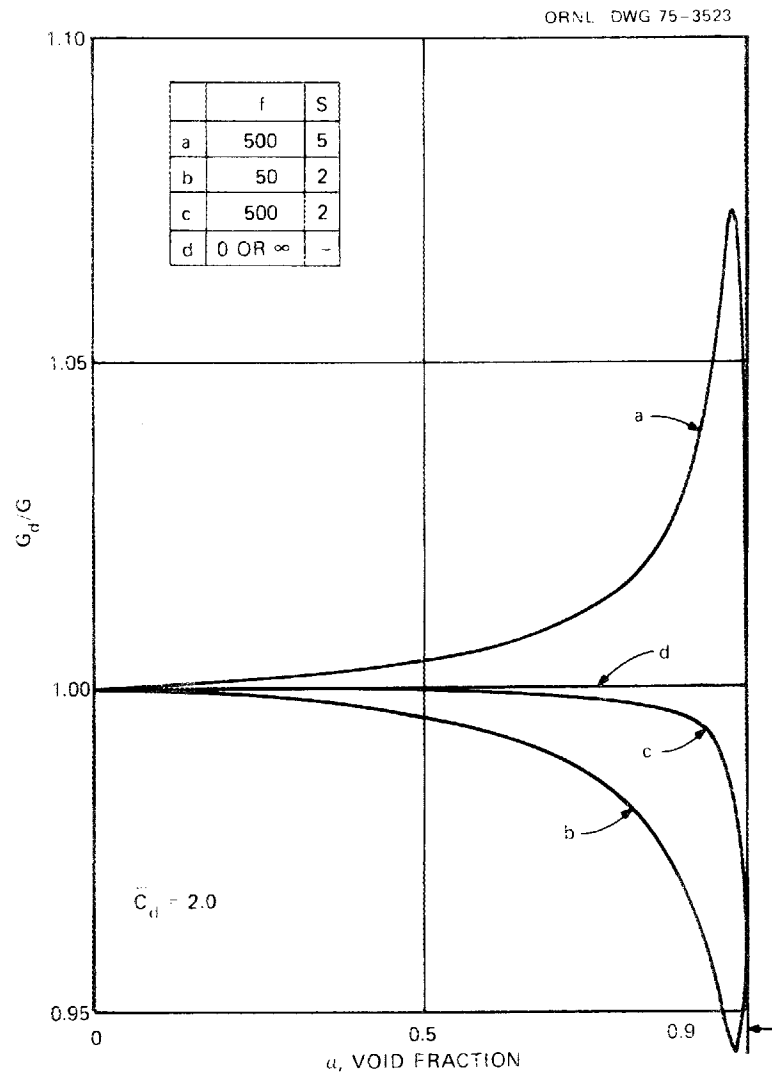


Fig. 29. Ratio of mass fluxes based on INEL method for drag disk and densitometer (G_d) and proposed model (G) for selected values of f and S [Eq. (29a)] and $\bar{C}_d = 2.0$.

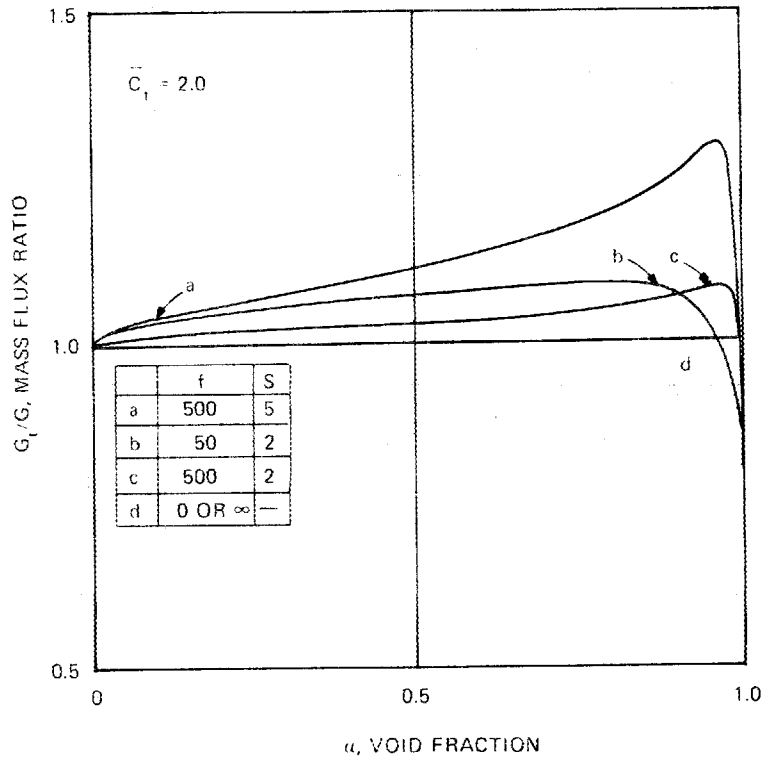


Fig. 30. Ratio of mass fluxes based on INEL method using turbine meter and densitometer (G_t) and proposed model (G) vs void fraction for selected values of f and S [Eq. (30a)] and $\bar{C}_t = 2.0$.

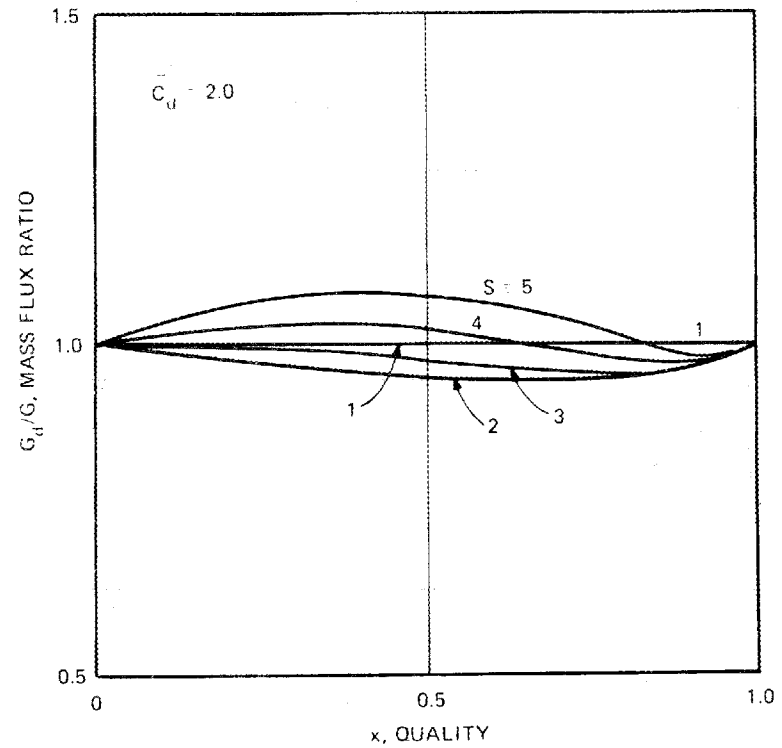


Fig. 31. Ratio of mass fluxes based on INEL method using drag disk and densitometer (G_d) and proposed model (G) vs quality for selected values of f and S [Eq. (29b)] and $\bar{C}_d = 2.0$.

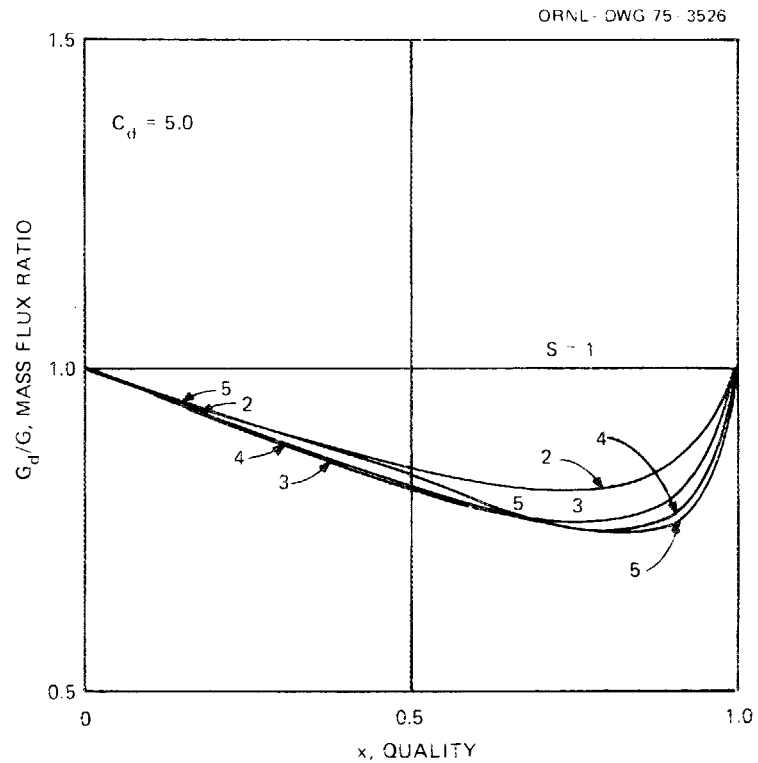


Fig. 32. Ratio of mass fluxes based on INEL method using drag disk and densitometer (G_d) and proposed model (G) vs quality for selected values of f and S [Eq. (29b)] and $\bar{C}_d = 5.0$.

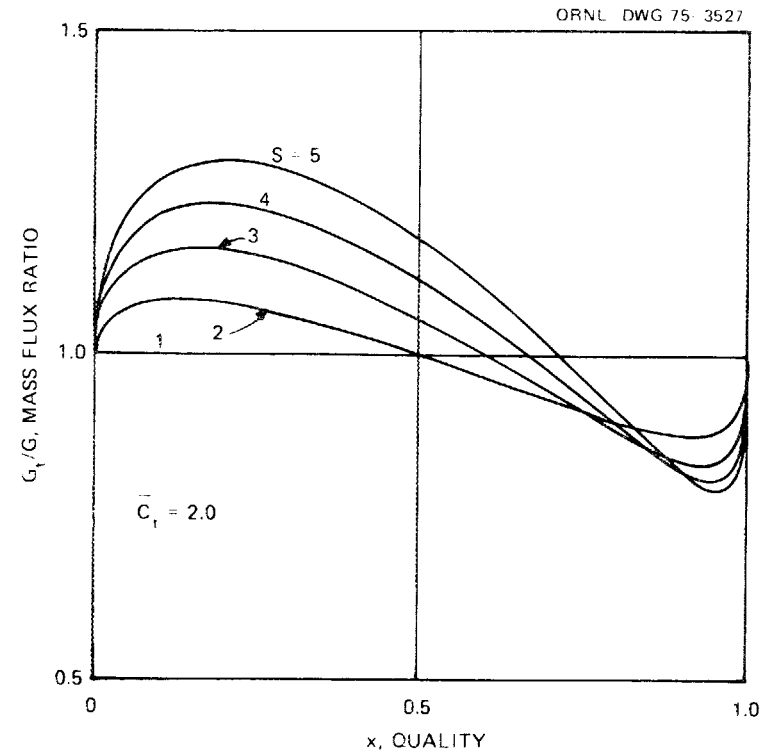


Fig. 33. Ratio of mass fluxes based on INEL method using turbine meter and drag disk (G_t) and proposed model (G) vs quality for selected values of S [Eq. (30b)] and $\bar{C}_d = 2.0$.

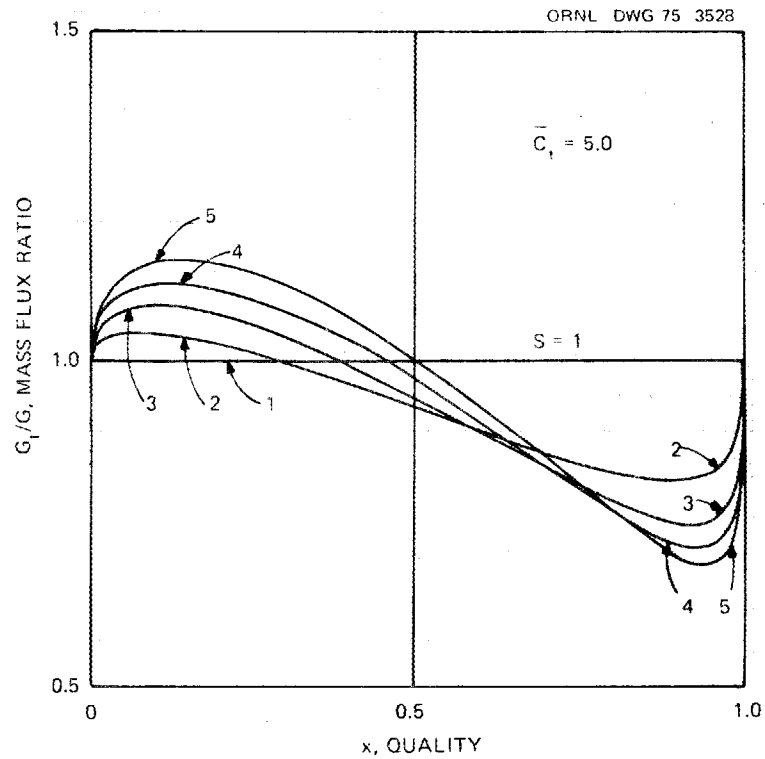


Fig. 34. Ratio of mass fluxes based on INEL method using turbine meter and densitometer (G_t) and proposed model (G) vs quality for selected values of S [Eq. (30b)] and $\bar{C}_t = 5.0$.

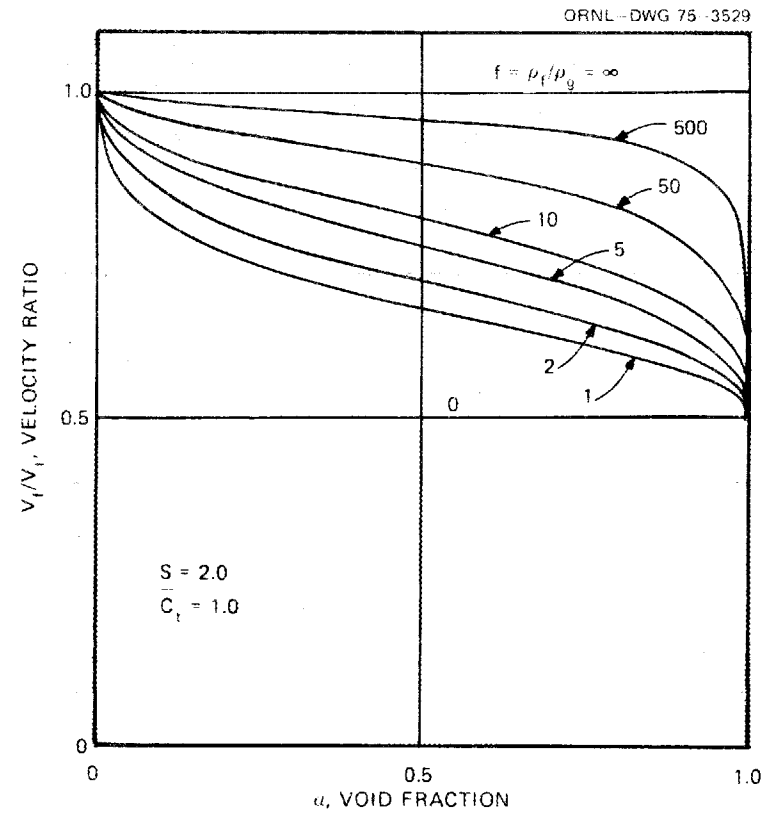


Fig. 35. Ratio of liquid phase velocity to turbine meter apparent velocity (= Popper's liquid phase velocity) based on proposed model [Eq. (34a)]; $S = 2.0$ and $\bar{C}_t = 1.0$.

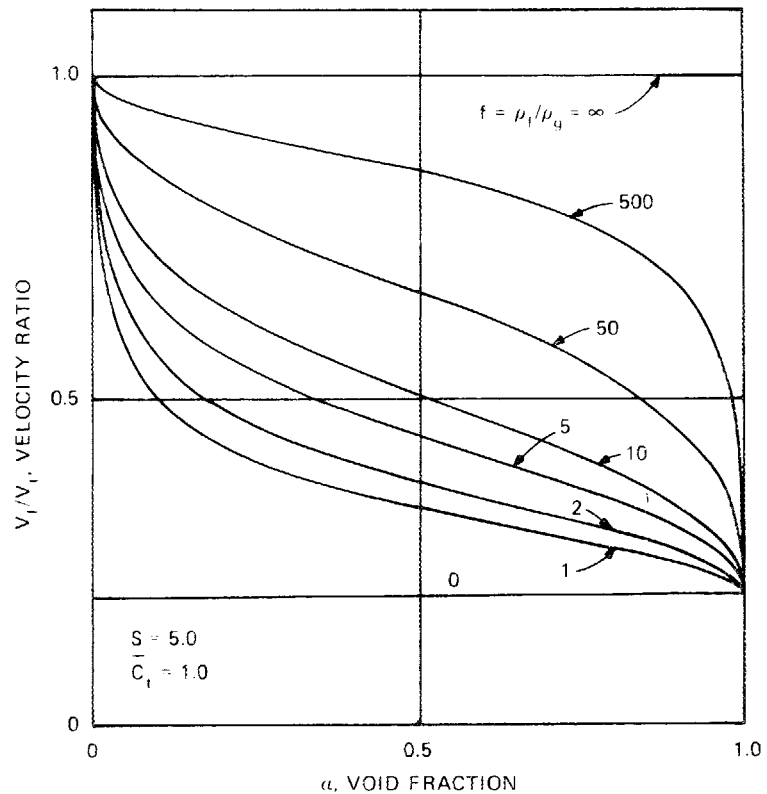


Fig. 36. Ratio of liquid phase velocity to turbine meter apparent velocity (= Popper's liquid phase velocity) based on proposed model [Eq. (34a)]; $S = 5.0$ and $\bar{C}_t = 1.0$.

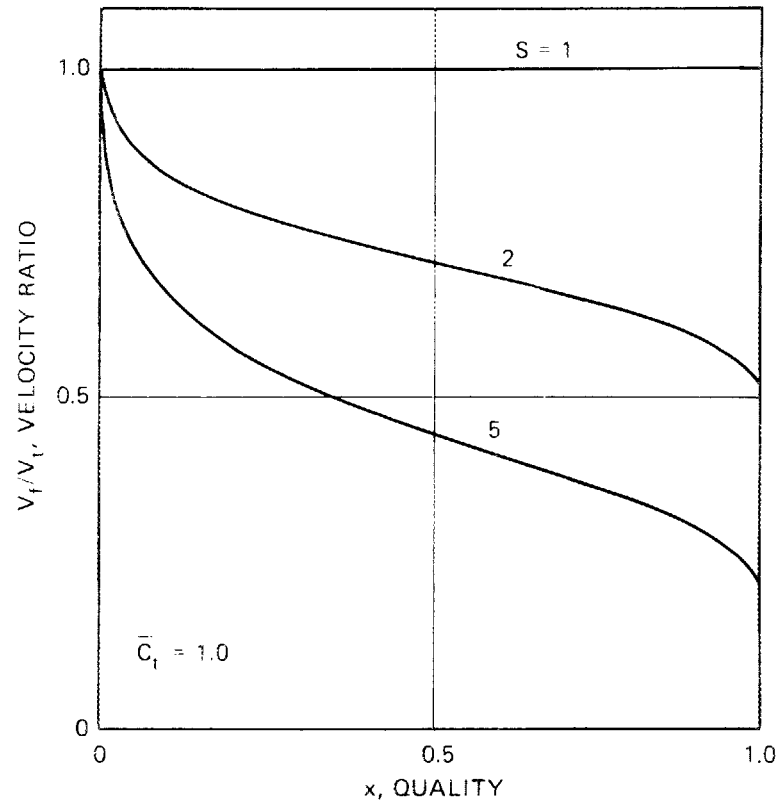


Fig. 37. Ratio of liquid phase velocity to turbine meter apparent velocity (= Popper's liquid phase velocity) based on proposed model [Eq. (34b)]. When V_f/V_t is expressed as a function of quality, the density ratio f is eliminated; $\bar{C}_t = 1.0$.

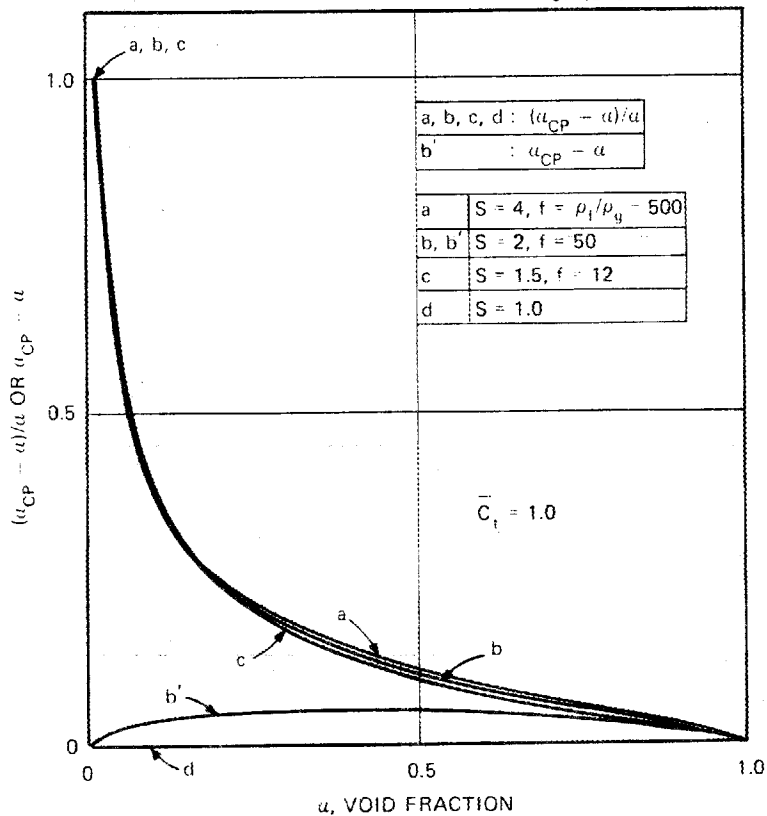


Fig. 38. Comparison of void fractions calculated through Popper's model (α_{CP}) and the proposed model (α) for selected values of f and S [Eq. (33)]; $\bar{C}_t = 1.0$.

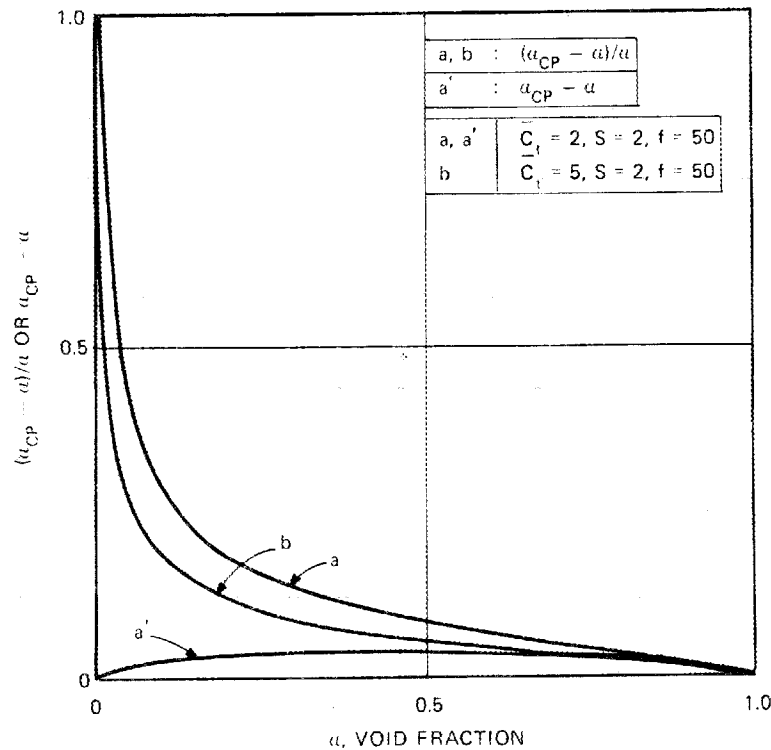
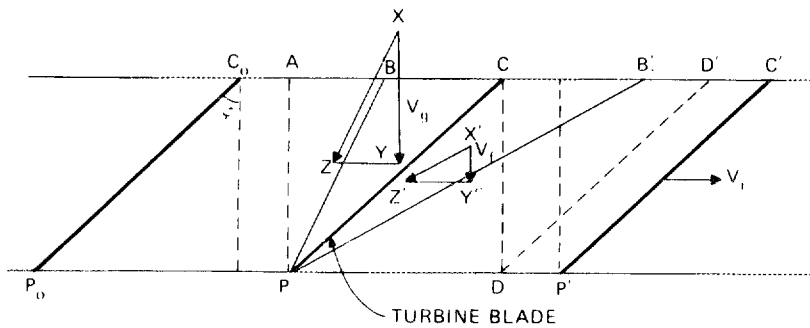


Fig. 39. Comparison of void fractions calculated through Popper's model (α_{CP}) and the proposed model (α) for selected values of S , \bar{C}_t , and f . Curves for $S = 4, f = 500$, and $S = 1.5, f = 12$ are similar to curve a if $\bar{C}_t = 2.0$; curve b is $\bar{C}_t = 5.0$ [Eq. (33)].



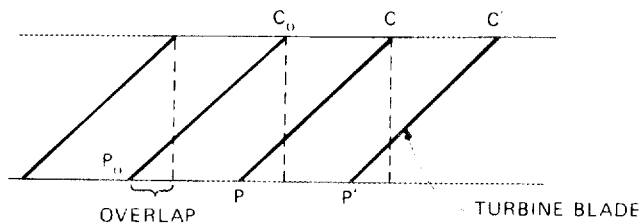
\vec{XZ} : ACTUAL VELOCITY OF STEAM TOWARD A TURBINE BLADE

$\vec{X'Z'}$: ACTUAL VELOCITY OF WATER TOWARD A TURBINE BLADE

$\vec{ZY} = \vec{Z'Y'} = \vec{V}_1, \vec{C_0C} = \vec{CC'}$

$\vec{XZ} \parallel \vec{BP}, \vec{X'Z'} \parallel \vec{B'P'}, \vec{CP} \parallel \vec{D'D}, \vec{C_0P_0} \parallel \vec{CP} \parallel \vec{C'P'}$

(a) TURBINE BLADES DO NOT OVERLAP (BASIS OF PROPOSED MODEL)



(b) TURBINE BLADES OVERLAP (AS OVERLAP INCREASES THE MOMENTUM BALANCE SHOULD APPROACH THE ROUHANI MODEL)

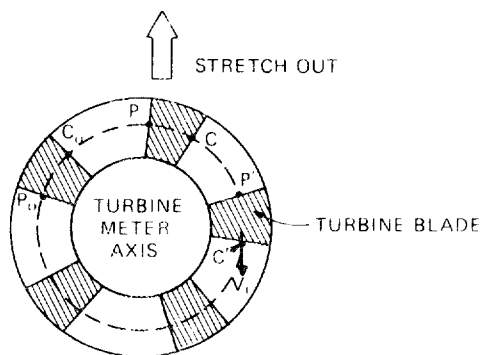


Fig. 40. Detailed sketch of velocity vectors about a turbine blade and comparison of turbine blade designs appropriate to Rouhani's model and the proposed model.

ORNL-DWG 75-3535

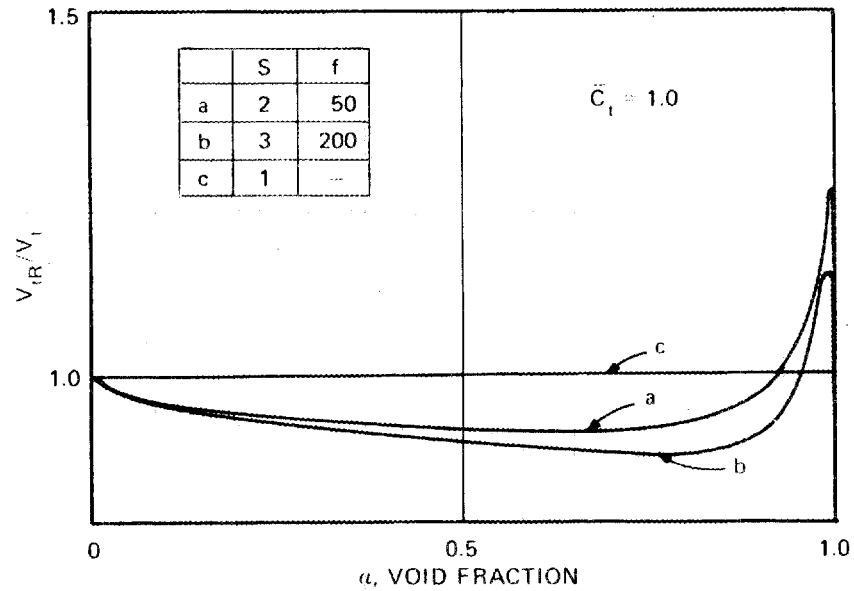


Fig. 41. Ratio of turbine meter velocities calculated with the Rouhani model (V_{tR}) and the proposed model (V_t) vs void fraction for selected values of f and S [Eq. (37a)]; $\bar{C}_t = 1.0$.

ORNL-DWG 75-3536

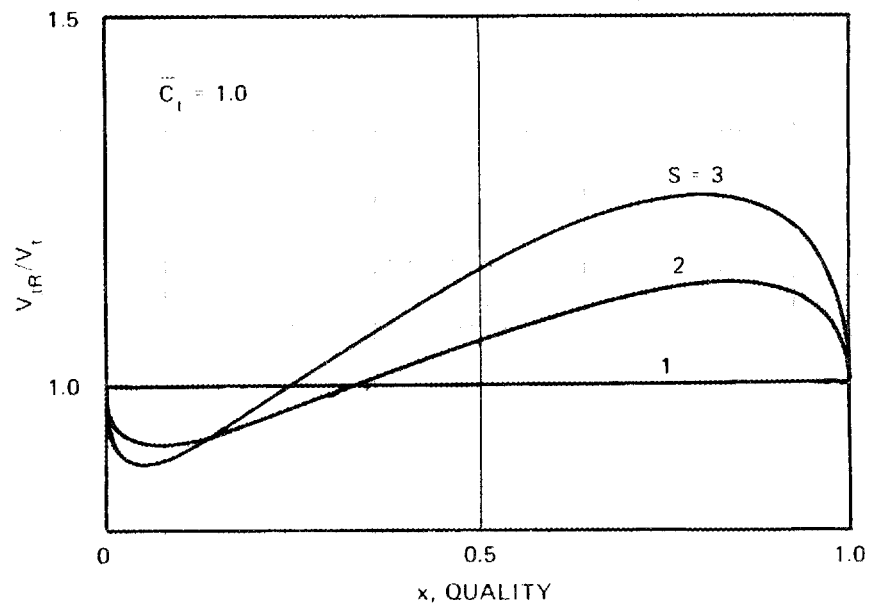


Fig. 42. Ratio of turbine meter velocities calculated with the Rouhani model (V_{tR}) and the proposed model (V_t) vs quality for selected values of S [Eq. (37b)]; $\bar{C}_t = 1.0$.

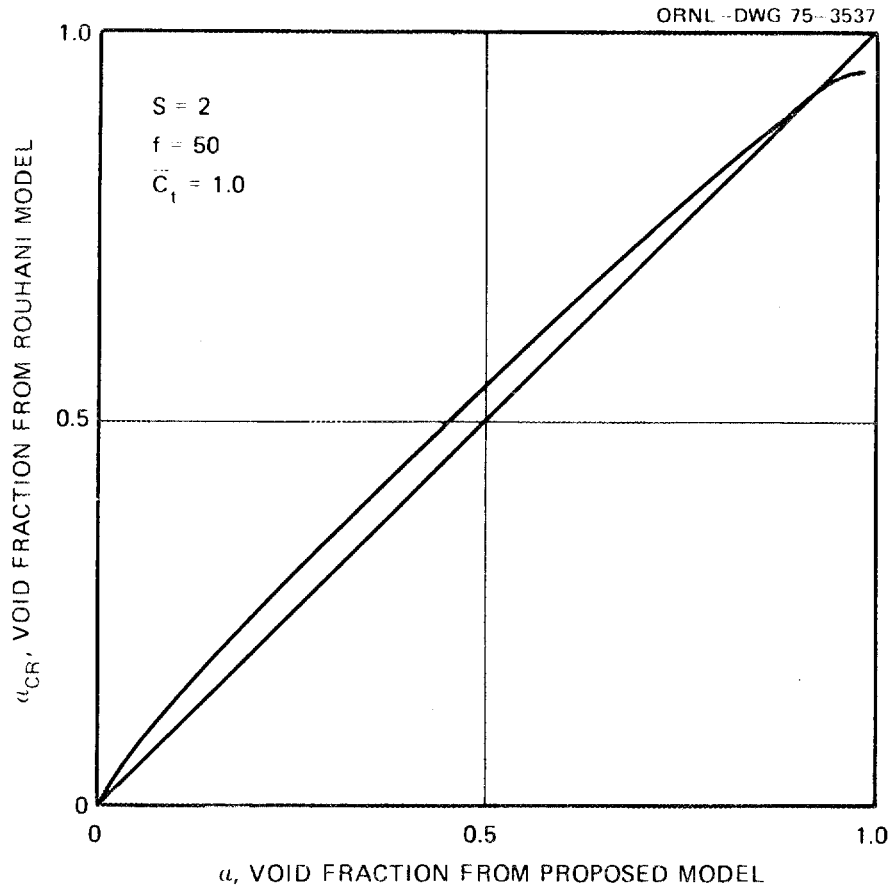


Fig. 43. Comparison of void fractions from Rouhani model (α_{CR}) and from proposed model (α) for $S = 2$, $f = 50$, $\overline{C}_t = 1$. The conditions $S = 3$, $f = 200$, $\overline{C}_t = 1$ yield almost the same curve.

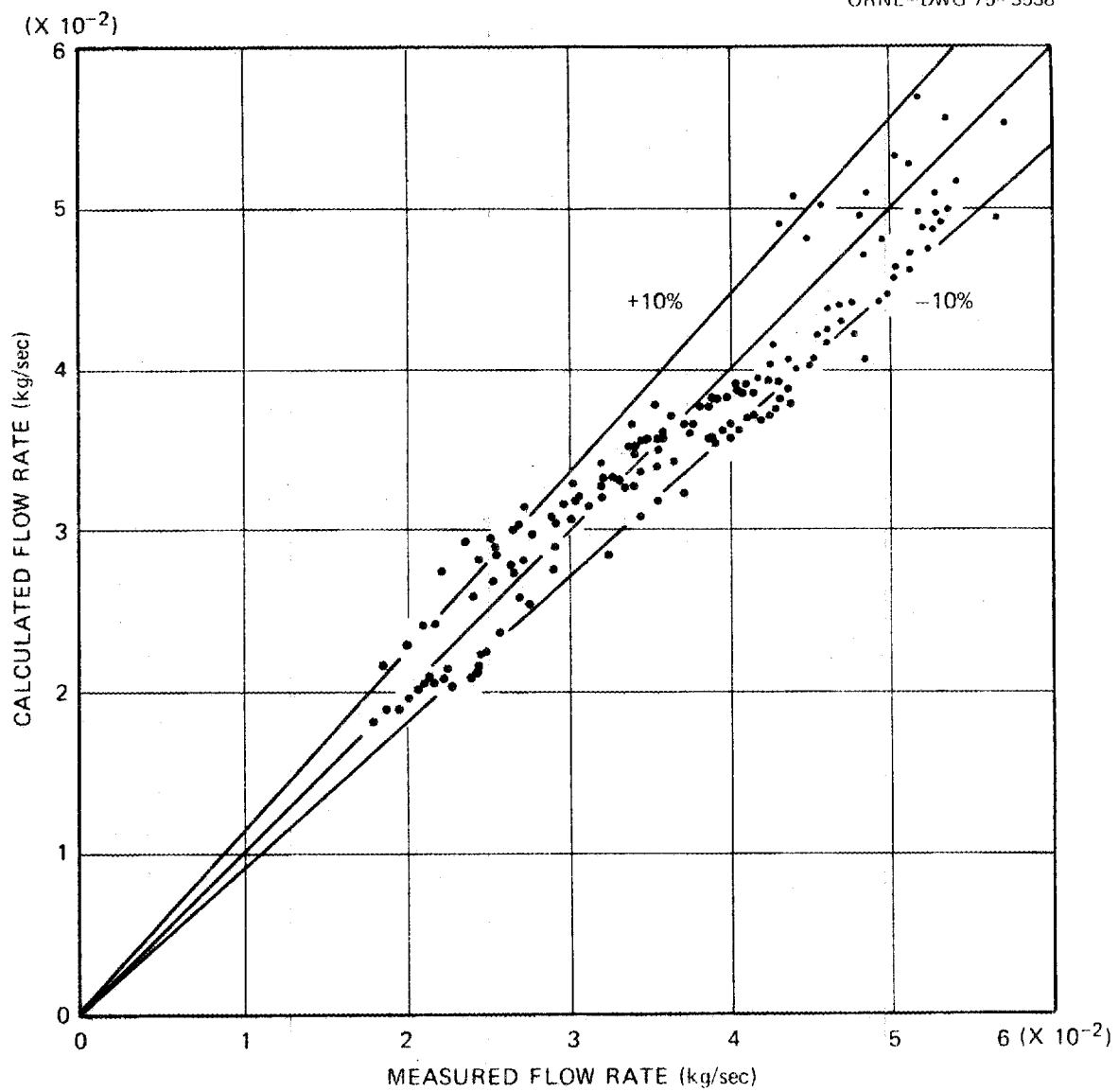


Fig. 44. Comparison of calculated flow rate by proposed model with Rouhani's measured flow rate.

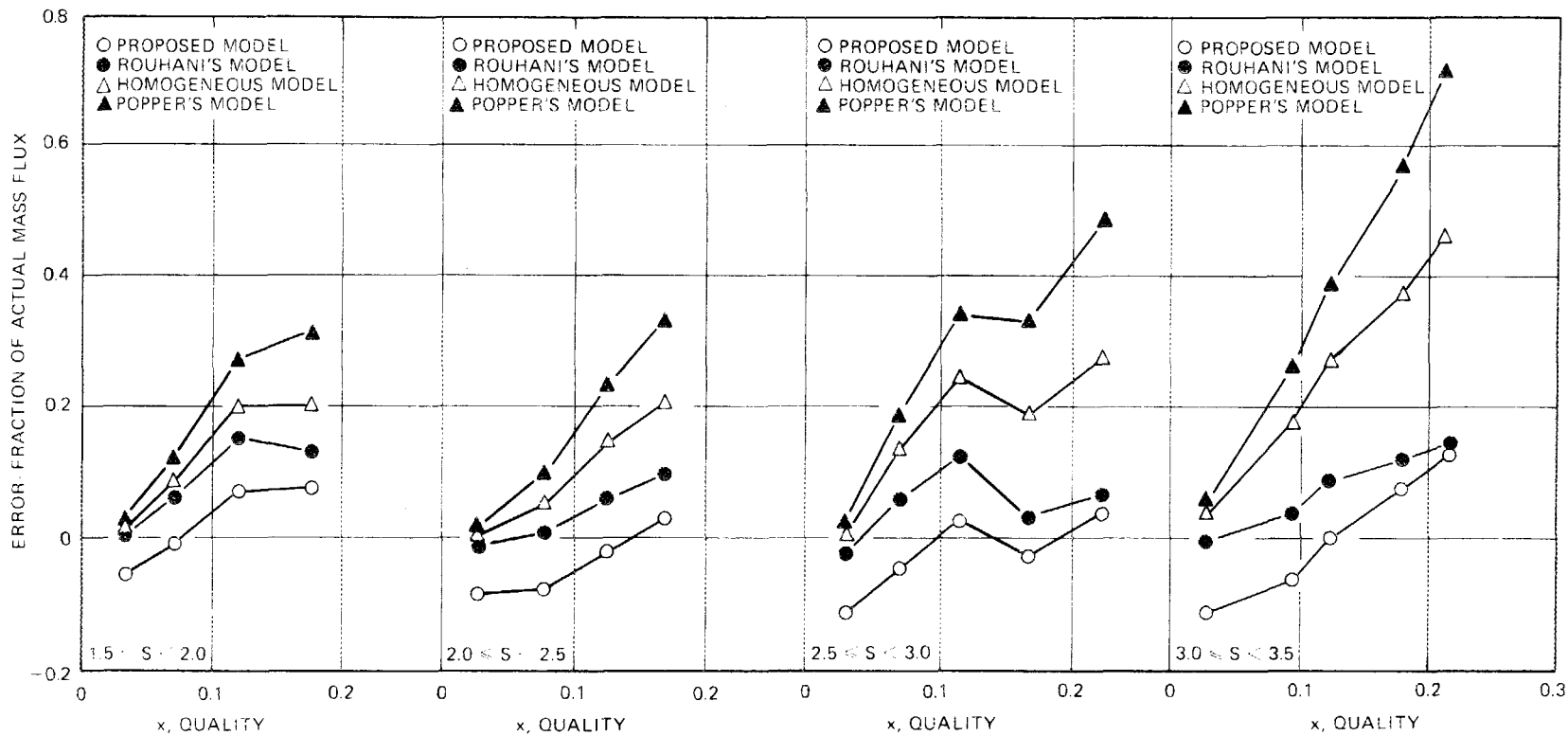


Fig. 45. Comparison of errors of four turbine meter models used in prediction of mass flow rate in the experimental data of Rouhani.

REFERENCES

1. B. Rüdiger et al., *Study of Processes During Blowdown of Water-Cooled Reactors*, Report 7 for the Federal Ministry of Education and Science Research Project RS16, Battelle, Frankfurt (June 1971).
2. D. B. Collins and M. Gacesa, "Measurement of Steam Quality in Two-Phase Upflow with Venturimeters and Orifice Plates," *Trans. ASME, J. Basic Eng.* 93, 11-21 (1971).
3. J. W. Murdock, "Two-Phase Flow Measurement with Orifices," *Trans. ASME, J. Basic Eng.* 84, 419-33 (1962).
4. R. James, "Metering of Steam-Water Two-Phase Flow by Sharp-Edged Orifices," *Proceedings of the Institution of Mechanical Engineers*, 180 (1965-1966).
5. D. Chisholm and J. M. Leishman, "Metering of Wet Steam," *Chem. Proc. Eng.* 50, 103-6 (1969).
6. D. Chisholm, "Flow of Compressible Two-Phase Mixtures through Throttling Devices," *Chem. Proc. Eng.* 48, 73-78 (1967).
7. J. R. S. Thom, "Prediction of Pressure Drop During Forced Circulation Boiling of Water," *Int. J. Heat Mass Transfer* 7, 709-24 (1964).
8. *Water Reactor Safety Research*, CKL-12-74, Aerojet Nuclear Company monthly report (November 1973).
9. O. Baker, "Simultaneous Flow of Oil and Gas," *J. Oil Gas* 53, 185-95 (1954).
10. E. R. Hosler, "Flow Patterns in High Pressure Two-Phase (Steam-Water) Flow with Heat Addition," *Chem. Eng. Prog. Symp. Ser.* 64, 54-66 (1968).
11. G. W. Govier and K. Aziz, *The Flow of Complex Mixtures in Pipes*, Van Nostrand, New York, 1972.
12. K. J. Baumeister, R. W. Graham, and R. E. Henry, "Momentum Flux in Two-Phase Two-Component Low Quality Flow," *A.I.Ch.E. Symp. Ser.* 69, 46-54 (1973).
13. P. M. Lang, "Information Concerning ANC Use of the Ramapo Flowmeters—PML-121-73," official correspondence from Aerojet Nuclear Company, June 1973.
14. G. F. Popper, *Lecture Notes on In-Core Instrumentation for the Measurement of Hydrodynamic Parameters in Water-Cooled Reactors* ANL-6452 (November 1961).

15. *Water Reactor Safety Research*, CKL-61-74, Aerojet Nuclear Company monthly report (December 1973).
16. G. F. Popper, "The Use of Turbine Type Flowmeters for the Determination of Exit Void Fraction in Reactor Core Subassemblies or Heat Transfer Facilities," Intralaboratory correspondence of the Argonne National Laboratory, February 1959.
17. G. F. Popper, *Proceedings of the Power Reactor In-Core Instrumentation Meeting*, Washington, D. C., TID-7598, pp. 37-47 (April 1960).
18. S. Z. Rouhani, "Application of the Turbine Type Flowmeters in the Measurements of Steam Quality and Void," *Symposium on In-Core Instrumentation*, Oslo, June 1974.
19. S. Z. Rouhani, *Application of the Turbine Type Flowmeters in Measurements of Steam Quality and Void*, RPL-683, AB Atomenergi, Studsvik (September 1963).
20. S. Z. Rouhani and K. M. Becker, *Measurements of Void Fractions for Flow of Boiling Heavy Water in a Vertical Round Duct*, AE-106 (September 1963).

INTERNAL DISTRIBUTION

- | | | | |
|-------|---------------------|--------|--------------------------------|
| 1. | A. H. Anderson | 39. | C. A. Mills |
| 2-11. | Izuo Aya | 40. | R. L. Moore |
| 12. | H. F. Bauman | 41. | F. H. Neill |
| 13. | C. J. Borkowski | 42. | L. Ott |
| 14. | R. H. Chapman | 43. | H. Postma |
| 15. | N. E. Clapp | 44. | J. L. Redford |
| 16. | W. B. Cottrell | 45. | R. C. Robertson |
| 17. | J. L. Crowley | 46. | J. P. Sanders |
| 18. | F. L. Culler | 47. | W. K. Sartory |
| 19. | D. G. Davis | 48. | Myrtle Sheldon |
| 20. | B. C. Duggins | 49. | J. D. Sheppard |
| 21. | B. G. Eads | 50. | I. Spiewak |
| 22. | G. G. Fee | 51. | R. S. Stone |
| 23. | M. H. Fontana | 52. | R. D. Stulting |
| 24. | A. P. Fraas | 53. | J. J. Taylor |
| 25. | J. H. Freels | 54-63. | D. G. Thomas |
| 26. | M. J. Goglia | 64. | D. B. Trauger |
| 27. | R. A. Hedrick | 65. | K. G. Turnage |
| 28. | R. E. Helms | 66. | J. D. White |
| 29. | H. W. Hoffman | 67. | M. D. White |
| 30. | O. H. Klepper | 68. | G. D. Whitman |
| 31. | C. G. Lawson | 69. | W. J. Wilcox |
| 32. | R. N. Lyon | 70. | L. V. Wilson |
| 33. | R. E. MacPherson | 71. | M. C. Wynn |
| 34. | C. D. Martin | 72. | ORNL Patent Office |
| 35. | W. J. McCarthy, Jr. | 73-74. | Central Research Library |
| 36. | R. W. McClung | 75. | Document Reference Section |
| 37. | H. A. McLain | 76-78. | Laboratory Records Department |
| 38. | S. L. Milora | 79. | Laboratory Records, ORNL R. C. |

EXTERNAL DISTRIBUTION

- 80-87. Director, Division of Reactor Safety Research, Nuclear Regulatory Commission, Washington, D. C. 20555
88. Director, Reactor Division, ERDA, ORO
89. Director, Research and Technical Support Division, ERDA, ORO
- 90-400. Given distribution as shown under categories NRC-1, -2, -4